International Geology Review, Vol. 48, 2006, p. 585–618.

Devonian Sedimentary Environments and Provenance of the Qinling Orogen: Constraints on Late Paleozoic Southward Accretionary Tectonics of the North China Craton

ZHEN YAN,[1]

State Key Laboratory of Lithospheric Evolution, Institute of Geology and Geophysics, Chinese Academy of Sciences, P.O. Box 9825, Beijing 100029, China

ZONGQI WANG, QUANREN YAN, TAO WANG,

Institute of Geology, Chinese Academy of Geological Sciences, Beijing 100037, China

WENJIAO XIAO, JILIANG LI,

State Key Laboratory of Lithospheric Evolution, Institute of Geology and Geophysics, Chinese Academy of Sciences, P.O. Box 9825, Beijing 100029, China

FANGLIN HAN, JUNLU CHEN, AND YONGCHENG YANG

Shaanxi Insititute of Geology Survey, Xianyang 712000, Shaanxi, China

Abstract

The Qinling orogen of central China occupies a key position in East Asia, and is of fundamental importance in unraveling its tectonic evolution. Devonian sedimentary basins are located between the North Qinling arc and the Baishuijiang Devonian–Permian accretionary wedge. Paleocurrent indictors and petrological and geochemical analyses show that turbiditic and coastal sandstones and pyroclasts developed in paleo-forearcs. Sedimentation of conglomerates and associated turbiditic and pyroclastic rocks evidently was related to the development of the North Qinling orogen rather than the South China craton. Gravels in the conglomerates were derived predominantly from the North Qinling and partly from its basement.

Northward Devonian subduction and subsequent uplift caused successive forearc depocenters and associated facies belts to migrate southwards synchronously with sedimentation. Transpressive and transtensional faults segmented the basins into discrete half-graben sub-basins. Paleocurrent analysis adjacent to thrust faults demonstrates that thrust sheets crests were truncated by erosion and provided detritus for sub-basins. Shallow-marine and turbiditic depositional systems evolved in complex patterns to produce varied facies frameworks associated with complex subduction accretion. These facts, together with other geological and geochemical data, demonstrate that the North China craton grew southwards by arc-accretion processes from the end of the early Paleozoic to the beginning of the late Paleozoic, long before the integration of the North China and Yangtze cratons.

Introduction

THE QINLING OROGEN occupies a key position in the Chinese Central Orogenic Belt (Zhang G. et al., 1995, 1996) that extends from the Pamirs–West Kunlun to the Korean Peninsula and tectonically separates northern Precambrain blocks (Tarim, Sino-Korean craton, or North China block [NCB]) from southern blocks (such as the South China block [SCB]) (Fig. 1) (Li C., 1976; Li C. et al., 1978; Mattauer et al., 1985; Zhang G. et al., 1989, 1995; Matte et al., 1996; Meng and Zhang, 1999, 2000; Xiao et al., 2002a, 2002b, 2003; Ratschbacher et al., 2003; Roger et al., 2003; Schwab et al., 2004). Consequently, the geology and tectonic evolution of the Qinling orogen are critical for a better understanding of the evolution and assembly of Asia.

Nevertheless, despite its great importance, the geology and the tectonic evolution of the Qinling orogen are still poorly understood. Although it is widely accepted that the orogen was finally consolidated in the early Mesozoic (Li S. et al., 1989, 1993; Okay et al., 1993; Yin and Nie, 1993; Hacker et al., 1998; Ames et al., 1993; Ye et al., 2000), its

[1]Corresponding author; e-mail: yanzhen@mail.igcas.ac.cn

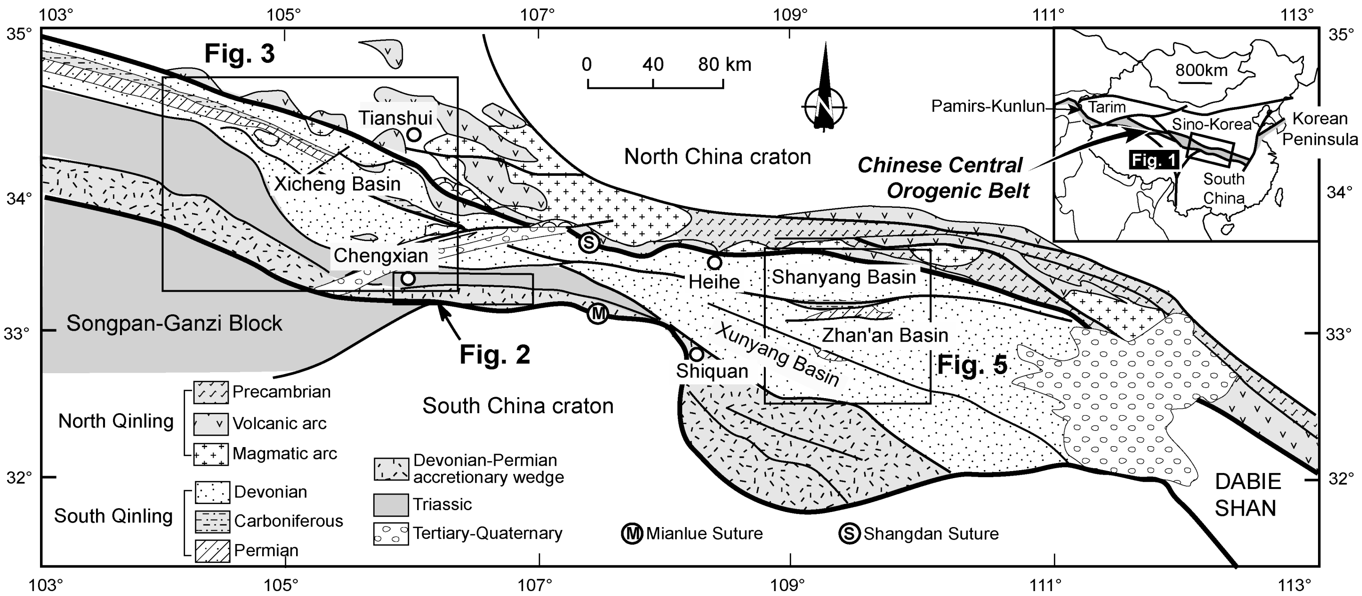

FIG. 1. Simplified geological map of the Qinling orogen (modified after Zhang E. et al., 1993; Liang, 1994; Zhou D. et al., 1995; Song Z. et al., 1996; Wang Z. Q. et al., 1999, 2002). The Shangdan suture separates the Qinling orogen into the North and South Qinling belts. Insert is a schematic map of China showing the position of the Chinese Central Orogenic Belt in grey, and the position of Figure 1.

Paleozoic history is much debated, and in particular the Devonian paleogeography (Mattauer et al., 1985; Zhang G. et al., 1989, 1995; Meng and Zhang, 1999, 2000; Ratschbacher et al., 2003). Several systematic studies have been undertaken on the evolution of the Qinling orogen, including the crystalline rocks (Li C. et al., 1978; Mattauer et al., 1985; Zhang H. et al., 1997; Huang and Wu, 1992; Zhang G. et al., 1989, 1995; Meng and Zhang, 1999, 2000; Ratschbacher et al., 2003). However, little has been done on the Devonian sedimentary rocks in this huge mountain range (Du D., 1986; Du Y., 1997). This paper presents the results of joint systematic research on the sedimentary environments and provenance of the Devonian strata in order to better understand the tectonic evolution of the orogen.

In the Qinling orogen, Devonian rocks crop out predominantly in the Xichen, Shanyang, Zhen'an, and Xunyang areas (Fig. 1). Abundant Pb-Zn deposits in carbonates have attracted considerable interest since the late 1960s. Some Chinese researchers studied the sequence stratigraphy and sedimentary environments of the basins, but they only focused on the reservoir characteristics, aiming to prospect the ore-bodies (Zhou Z. et al., 1992; Fang et al., 2001; Cao et al., 1990). Nevertheless, detailed, systemic studies of the sedimentary environments and tectonic settings have yet to be made. At present, new studies are required to reconcile differences between the Devonian clastic rocks and the ages of ophiolites, paleomagnetic data, and deformational and metamorphic history. An accurate understanding and interpretation of the provenance and tectonic setting of the Devonian sedimentary rocks is essential to reconstruct the Paleozoic evolution of both the NCB and SCB.

In this paper, we first briefly review the main tectonic units of the Qinling orogen, and present a detailed description of the Paleozoic forearc basins, which is the main target of this paper. The composition of sandstones and source settings are discussed in relation to our new detrital, paleocurrent, and geochemical data. Finally, we provide new evidence for the tectonic environment of the basins in the orogen, and discuss the Paleozoic accretion tectonics along the southern margin of the NCB.

Geological Framework

The Qinling orogen (Fig. 1) is a well-preserved example of a Paleozoic and Mesozoic collisional belt in which early Paleozoic intra-oceanic island arcs and Silurian–Devonian magmatic arcs accreted to the southern margin of NCB in the Devonian (Mattauer et al., 1985; Yan, 1985; Zhang G. et al., 1989; Lerch et al., 1995; Xue et al., 1996a, 1996b; Meng and Zhang, 1999, 2000; Ratschbacher et al., 2003; Zhang H. et al., 1997). The Shangdan and Mianlue sutures separate the orogen into three main tectonic units (Zhang G. et al., 1995; Meng and Zhang, 1999, 2000): North Qinling, South Qinling, and northern marginal belt of the SCB. Recently, a Devonian–Permian accretionary wedge was defined along the southern margin of the NCB (Wang Z. Q. et al., 1999, 2002; Yang, 1999; Wang, T., 2003; Ratschbacher et al., 2003). Devonian–Permian sedimentation took place between the island arc and the accretionary wedge.

Shangdan and Mianlue sutures

The Shangdan suture along the Shangdan fault records a middle Paleozoic collisional event that resulted from the closure of the paleo-ocean between the North and South Qinling (Mattauer et al., 1985; Zhang G. et al., 1995), which is represented by discretely exposed arc-related ophiolitic rocks, forearc sediments, subduction- and collision-related granites, and a complex ductile-brittle fault system (Zhang G. et al., 1989; Meng et al., 1997; Yu and Meng, 1997). Granitoids within the Shangdan fault with a $^{207}Pb/^{206}Pb$ single zircon age of 383 ± 8 to 345 ± 11 Ma resulted from underthrusting of oceanic crust beneath the NCB in the Devonian (Zhang H. et al., 1997). The early history of the Shangdan fault can be traced back to the middle–late Proterozoic when rifting was active (Zhang G. et al., 1988). Mattauer et al. (1985) provided evidence for ~ 315 Ma sinistral strike-slip faulting within this suture. Mica schist has a $^{40}Ar/^{39}Ar$ age of 355.09 ± 4.44 Ma on biotite (Li J. et al., 1997), suggesting that tectonic activity took place along the suture in the Early Carboniferous. In the Triassic, the Shangdan fault was reactivated by several stages of intracontinental thrusting and strike-slip faulting (Ratschbacher et al., 2003).

The Mianlue suture was the product of the closure of the Qinling Ocean between the South Qinling and SCB in Late Triassic time (Meng and Zhang, 1999, 2000). Oceanic relics, arc-related volcanic blocks, and sedimentary blocks occur along this suture. Imbricate thrusts and associated folds are characteristic. Devonian turbidites, Early Carboniferous radiolarian chert (Feng et al., 1996), and Rb/Sr isochrons and Sm/Nd whole-rock of 241

± 4.4 and 220.2 ± 8.3 Ma from volcanic rocks (Li S., 1994), all suggest that the Qinling Ocean existed during the Devonian–Carboniferous and was closed in the Triassic. Recent studies suggest that the Mianlue suture resulted from final subduction and accretion along the southern margin of the NCB (Ratschbacher et al., 2003).

North Qinling arc

The North Qinling is mainly composed of an early Proterozoic Qinling arc, intensively deformed and metamorphosed to high grade, and two zones of early Paleozoic (~490–470 Ma) intra-oceanic arc-type ophiolites (the Danfeng and Heihe units) and backarc rocks (Erlangping unit) (Zhang Z. et al., 1994; Sun et al., 1996; Xue et al., 1996a, 1996b; Zhang et al., 1988; Li et al., 1989). The North Qinling is widely interpreted as a mid-Paleozoic orogen (Mattauer et al., 1985) that contains an arc that accreted to its southern margin (Yan, 1985; Zhang B. et al., 1994; Lerch et al., 1995; Zhang H. et al., 1997; Zhai et al., 1998).

Trondjhemite, tonalitie, gabbro, and monzonitic granite are abundant (Huo and Li, 1995; Xue et al., 1996a) in the North Qinling. Plutons cutting the Proterozoic Qinling arc are granites and granodiorites with initial $^{87}Sr/^{86}Sr$ ratios ≥ 0.707, whereas those cutting the Erlangping unit are gabbro-quartz monzodiorites with initial $^{87}Sr/^{86}Sr$ ratios ≥ 0.706 (Xue et al., 1996a), implying that the magmas were influenced by their crustal substrate. Plutons cutting these units have yielded U/Pb zircon ages of 422 ± 14, 410 ± 11, 406 ± 4, 401 ± 14, 414 ± 4 and 395 ± 6 Ma (Lerch et al., 1995), 307 ± 5, and 308 ± 5 Ma (Song Z. et al., 1996); Pb/Pb zircon ages of 397 (Reischmann et al., 1990) and 402 Ma (Xue et al., 1996a); Rb/Sr isochrons of 430, 396, and 399 Ma (Huo and Li, 1995), 403 ± 17 (Li S. et al., 1989), and 383 ± 8 Ma (Li X. et al., 1992); $^{40}Ar/^{39}Ar$ hornblende ages of 402 and ~400 Ma (Ratschbacher et al., 2003); and K/Ar ages of 324, 349, 408, and 420 Ma (Huo and Li, 1995). Trace- and rare earth–element analyses of granites are consistent with the interpretation that the plutons developed within a Devonian batholithic arc above a north-dipping subduction zone (Yan, 1985; Huo and Li, 1995; Lerch et al., 1995; Xue et al., 1996a, 1996b; Zhang H. et al., 1997; Zhai et al., 1998; Zhou D. et al., 1995). These data imply that an Andean-type continental magmatic arc was built, starting in the Late Silurian, and a sedimentary basin developed in the suture along the flanks of the arc.

The host rocks of the Devonian batholith were affected by "regional contact metamorphism" in the mid-crust of the magmatic arc (Hu et al., 1993; Zhai et al., 1998). Metamorphic mineral ages of this "regional contact metamorphism" include 404 ± 5 Ma $^{40}Ar/^{39}Ar$ on hornblende (Zhai et al., 1998) and 421 ± 2 Ma (Li and Sun, 1995) on Erlangping amphibolite; 404 ± 2 Ma on Qinling granulite (Zhai et al., 1998); 420 ± 30 Ma on amphibolite at Songshugou (Ratschbacher et al., 2003) and 401 (Niu et al., 1994) on hornblende; $^{40}Ar/^{39}Ar$ (on biotite) of 355.09 ± 4.44 Ma on a Danfeng mica schist (Li J. et al., 1997); eight K/Ar muscovite and biotite ages on Qinling unit metamorphic rocks that range from 480 to 354 Ma (Zhang Z. et al., 1991; RGS Henan, 1989); and one Rb/Sr whole-rock isochron on a greenschist-facies pillowed basalt of 402 ± 6 Ma (Sun et al., 1996). These isotopic data demonstrate that granitic intrusions with arc characteristics did not end in the Carboniferous.

Baishuijiang accretionary wedge

In the Chengxian and Shiquan areas, a suite of turbidites with thin chert interlayers, carbonates, and volcanic and pyroclastic rocks (BGM. Shaanxi, 1994, 1999; Figs. 1 and 2) was named after the "Baishuijiang Group," and have been regarded as Silurian in age since the 1930s (Ye and Guan, 1944; Li J. et al., 1994; Zhang E. et al., 1993). Volcanic blocks include calc-alkaline basalt, basaltic dacite, andesite, andesitic tuff and lava, and basalt blocks near Kangxian yielded a zircon SHRIMP age of 812 ± 22 Ma (Wang T., 2003). *Cldopora palaeogracilis Tchi*, *Thamnopora* sp., *Paraortnograptus* sp., *Productus* sp., *Marginifera visceniana*, and small-shelly fossils occur in some limestone blocks (BMG Gansu, 1982; BGM Shaanxi, 1994), demonstrating that they contain Cambrian, Ordovician, Devonian, and Carboniferous fauna. *Follicucullus* sp., *Albaillella aff. Levis*, *Srakaeopshaera* sp., *Albaillella excelsa, aff. Levis*, *Follicucullus charveti*, *Pseudoalbaillella lomentaria*, *Albaillella* sp., *Albaillella triangularis*, *Follicucullus* sp., and *Radiolaria* sp. were also separated from thin-bedded limestone and chert (Wang T., 2003). The geochemical character of the mudstone and sandstone matrix implied that they were deposited in front of a continental arc (Wang T., 2003). The different blocks with different ages and tectonic settings demonstrate that they belong to a mélange.

Farther east, the "Baishuijiang Group" is juxtaposed against a Carboniferous–Permian Shiquan

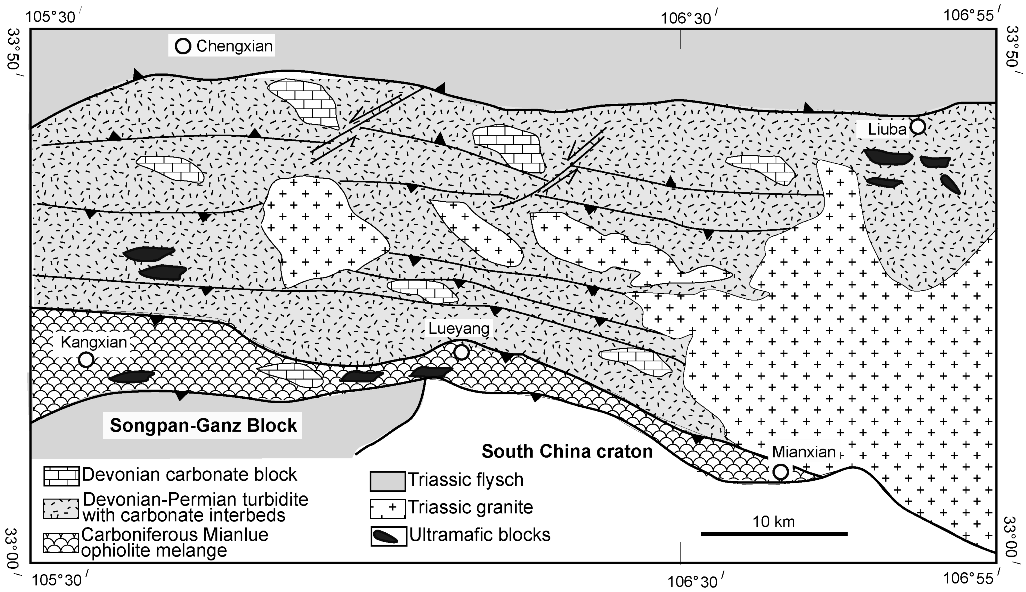

FIG. 2. Geological map of the Devonian-Permian accretionary wedge in the Kangxian, Lueyang, and Mianxian areas (modified after Wang Z. Q. et al., 1999, 2002; Wang T., 2003; Yang, 1999).

accretionary wedge (Fig. 1), which is defined in the Shiquan area by its rock assemblages, deformation styles, sedimentary environments, and fossils (Wang Z. Q. et al., 1999, 2002). These rocks belong to the Silurian–Permian Mianlue ophiolite mélange along the southern margin of the NCB.

Late Paleozoic Forearc Basins

Basement of the basins

Devonian sediments unconformably overlie the early Paleozoic and Precambrian strata. The Shangdan fault separates these basement rocks into two parts with different tectonic settings. The northern part is dominantly composed of island-arc volcanic rocks, which include the Danfeng, Luohansi, and Liziyuan units (Wang Z. Q. et al., 2002). The Danfeng unit consists of pillow lava, andesite, tuff, and tuffaceous clastic rocks with an island-arc signature based on geochemical analysis (Zhang Z. et al., 1994; Lerch et al., 1995). A Sm-Nd whole-rock age of 914–1015 Ma (Zhang Z. et al., 1996) and Ordovician–Silurian radiolarian fossils (Cui et al., 1996) were obtained from this unit. The Liziyuan unit consists of pillow lava, andesite, felsic volcanic rocks, clastic rocks, and marble metamorphosed under low hornblende and greenschist-facies condition; they formed in an island-arc setting (Song et al., 1991; Zhang W. and Meng, 1994). Cambrian–Devonian spore and conodontophoridia fossils were separated from a marble (Li Y., 1988). The Luohansi unit consists of calc-alkaline basalt, andesitic basalt, andesite, and dacite without any reliable age. Geochemical studies indicate these rocks were generated in an island-arc setting near an active continental margin (Xiao P. et al., 1999).

The southern part of the basement consists of Precambrian, Cambrian, Ordovican, and Silurian rocks. Pre-Cambrian basement mainly consists of volcanic rocks that formed in island-arc, backarc, and rift settings (Zhao et al., 1995; Wang S., 1995; Zhou D. et al., 1998). Cambrian–Ordovician carbonates that overlie the volcanic rocks formed in an archipelagic ocean (Yin and Huang, 1995). The Silurian series is dominated by turbidites with chert, carbonate, and mafic and ultramafic rocks. The above data suggest that the basement of the Devonian basins comprises oceanic crust, abundant carbonate islands, an island arc, and an accretionary wedge.

Structure of the basins

Faults separate the Devonian basin into several sub-basins (Fig. 1). Basin infills are early Devonian–Early Carboniferous turbidite interlayered with shallow-water sediments. In perpendicular zones to the trend of the orogenic belt, the infills become younger to the south. These characteristics imply that the Devonian palaeogeographic framework of the basins comprised alternating depressions and uplifts separated by faults. Synsedimentary thrusts that cut the strata and form duplex structures controlled the deposition and evolution of the basins, and played an important part in the formation of the ore deposits (Fang et al., 2001).

In the Xicheng Basin, the synsedimentary Gucheng-Shujiaba fault (F1) separated the Dacaotan Group (Upper Devonian) and the Shujiaba Group (Middle–Upper Devonian) (Wang Z. Q. et al., 2002; Figs. 3 and 4). Lenses of syntectonic breccia along the fault originated from the Dacaotan Group in the fault hanging wall, which suggests that the fault developed in the mid-Late Devonian. The Lixian-Mayanhe fault (F2) separates the turbidity deposits of the Shujiaba Group and the Xihanshui Group (early Upper Devonian). Upper Devonian and Carboniferous chert and limestone containing abundant radiolarian occur within the fault and in its footwall. However, the hanging wall consists of Carboniferous nonmarine sandstones and conglomerates with abundant plant fossils. This demonstrates that the fault controlled deposition of sediments in the Carboniferous. In the southern margin of the Xicheng Basin, the Minxian-Leiba arc-shaped thrust fault (F3) controlled sedimentation in the Permian and Triassic. To the north of the fault, Permian limestone, deposited in coastal environments, only crops out in small areas. Devonian–Triassic deep-water deposits crop out to the south of this fault. He (1996) demonstrated that the thrust fault controlled the slumping and occurrence of the Triassic turbidite. This demonstrates that the fault developed in the Permian and Triassic. These characteristics suggest that the faults developed from north to south and became younger southward, forming an imbricate thrust-fold system.

In the eastern part of the Qinling, faults within the basins have similar features as those in the Xicheng Basin (Figs. 5 and 6). The Heishan fault (F4) separates the Upper Devonian Tongyusi Formation and Middle–Upper Devonian Liuling Group, and it controlled the distribution of volcanic sediments. The Shanyang fault (F5) is a Middle Devonian synsedimentary fault that developed within the Middle Devonian Chigou Formation (Duanmu, 2000). The Banyan fault (F6) marks the boundary zone of the Xunyang and Zhen'an basins that controlled Carboniferous–Triassic sedimentation on both sides of it. To the northern part of this fault, Carboniferous nonmarine deposits are interbedded with coal beds containing plant fossils; Devonian–Triassic marine deposits occur to the south of the fault. The Shuanghe fault (F7) is a multiple structure, synchronous with the Xunyang Basin; it controlled the Devonian–Early Carboniferous sedimentation and depression during initial development of the basin.

Sedimentary Environments

Devonian deposits in the South Qinling largely consist of conglomerates, sandstones, siltstones, mudstones, and limestones. Their lateral extent and vertical successions are well known. Previous authors emphasized their lithological assemblages, and focused on the eastern part of this belt. But the sedimentary environments and rock assemblages in these basins are more complex than those in the Xicheng Basin. We summarize below their sedimentary features in order to illustrate changes in the sedimentary environments (Tables 1 and 2).

Xicheng Basin

The Devonian System of the Xicheng basin not only consists primarily of Middle–Upper Devonian strata (Figs. 3 and 4), but it also locally includes Lower Devonian strata. Lower Devonian outcrops near the Wujiashan and Leiba areas consist primarily of siltstone, mudstone, and thin-bedded limestone, but conglomerate, siltstone, and limestone with abundant fossil corals are present in the Wujiashan area (Li Y., 1989; Li J., 1994; Zhang E. et al., 1993; Zhang W. and Meng, 1994). The Middle Devonian strata are typified by the lower part of the Shujiaba Group and the Xihanshui Group in the Shujiaba and Xihe areas. Turbidite deposits are dominated by terrigenous clastic rocks intercalated with thin-bedded micrite and marls.

The Upper Devonian Dacaotan Group that occurs in the northern part of the basin contains *Leptophloeum rhombicum* Dawson (Fig. 3), has a maximum thickness of ~4000 m, and rests unconformably on the Danfeng unit (Cao et al., 1990; Zhang E. et al., 1993; Zhang W. and Meng, 1994). Matrix-supported conglomerates with sandstone interbeds show weakly inverse grading and crude cross-bedding (Fig. 7A). Clast-supported conglomerates are characterized by lenticular bedding and erosion surfaces. Sandstone drapes and imbricate clasts occur in the conglomerates. These are the

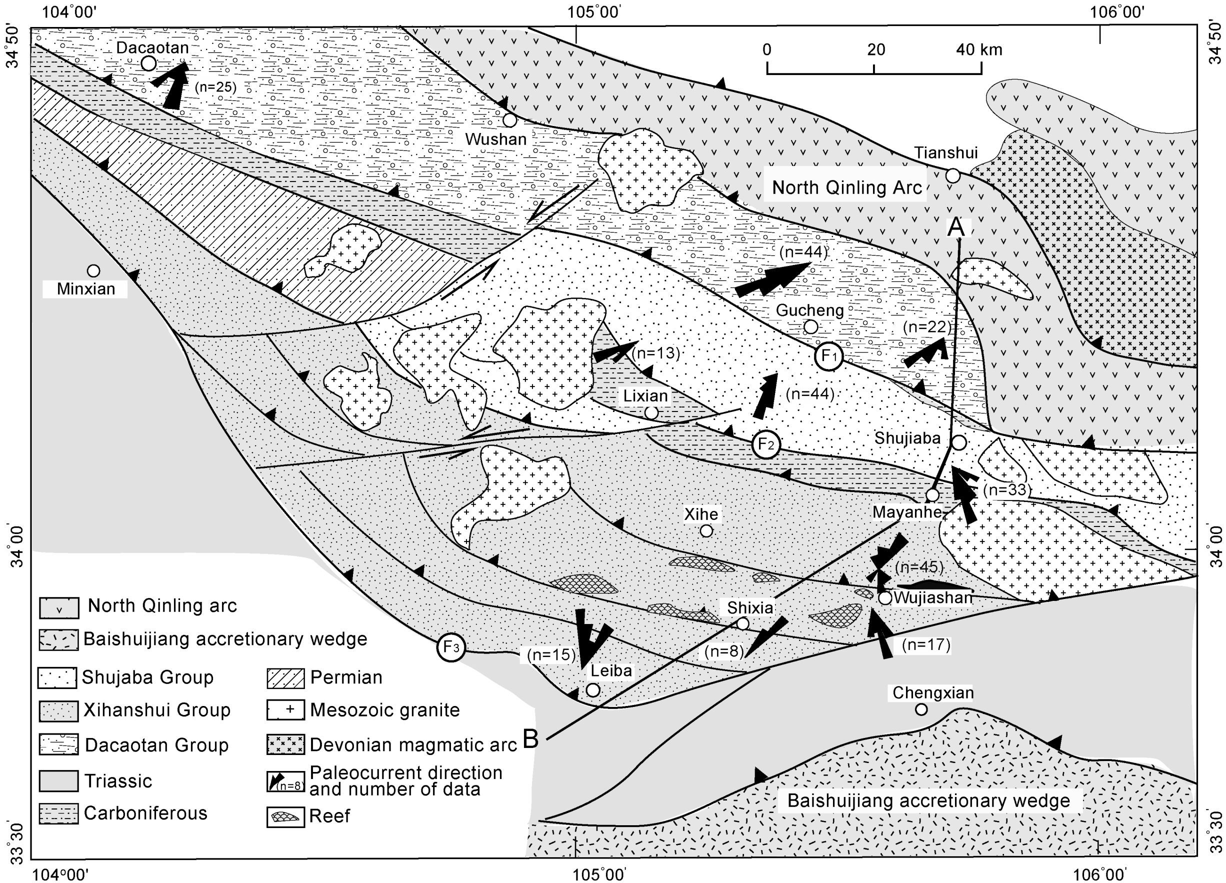

FIG. 3. Geological map and directional palaeocurrent data of the Xicheng Basin. Stratigraphic data from Li J. et al. (1994), Zhang E. et al. (1993), Zhang W. and Meng (1994) and Li Y. (1988, 1989). Reef data from Du Y, (1997). Symbols: F_1 = Gucheng-Shujiaba fault; F_2 = Lixian-Mayanhe fault; F_3 = Minxian-Leiba fault. Location of the structural cross-section of Figure 4 is marked as A–B.

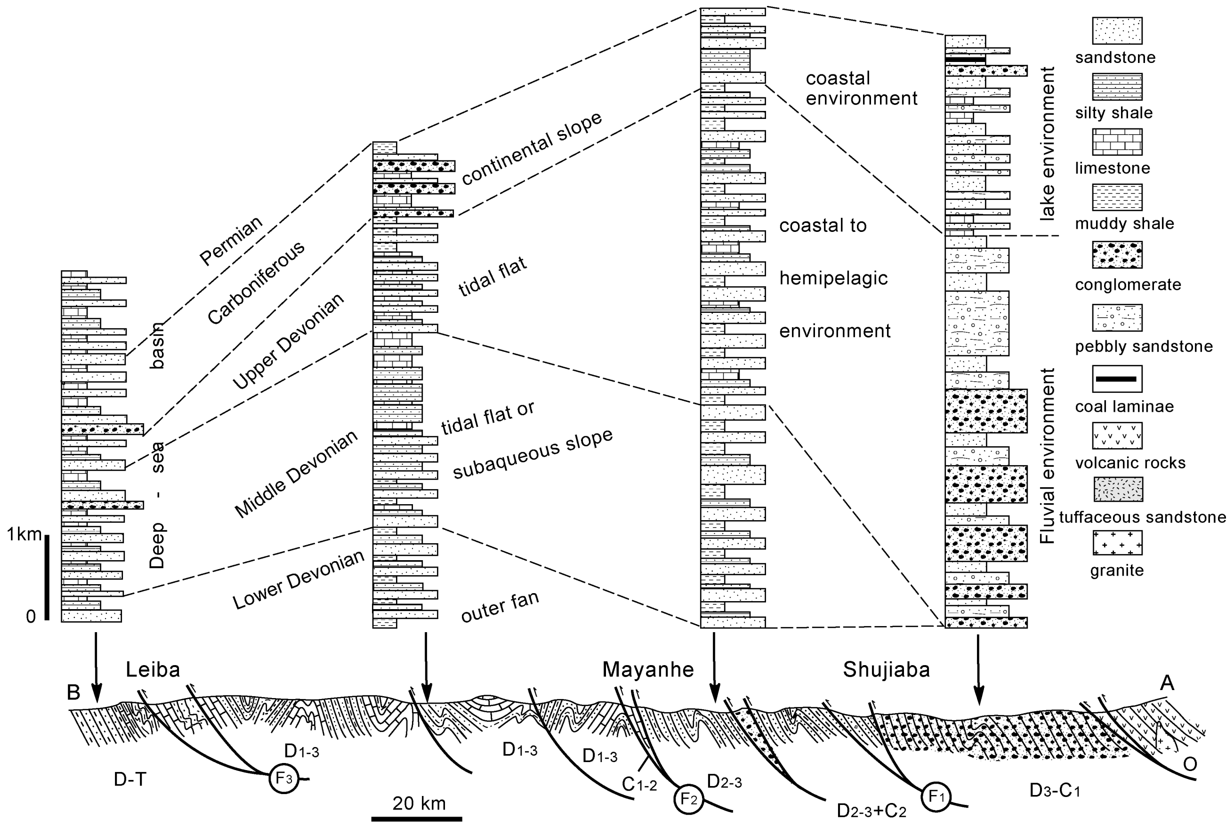

FIG. 4. Structural section and sedimentary columns of the Xicheng Basin. Stratigraphic data from Li J. et al. (1994). Symbols: D-T = Devonian–Triassic; D_{1-3} = Lower–Upper Devonian; C_{1-2} = Lower–Upper Carboniferous; D_{2-3} + C_2 = Middle–Upper Devonian and Upper Carboniferous; D_3 – C_1 = Upper Devonian–Lower Carboniferous; O = Ordovician.

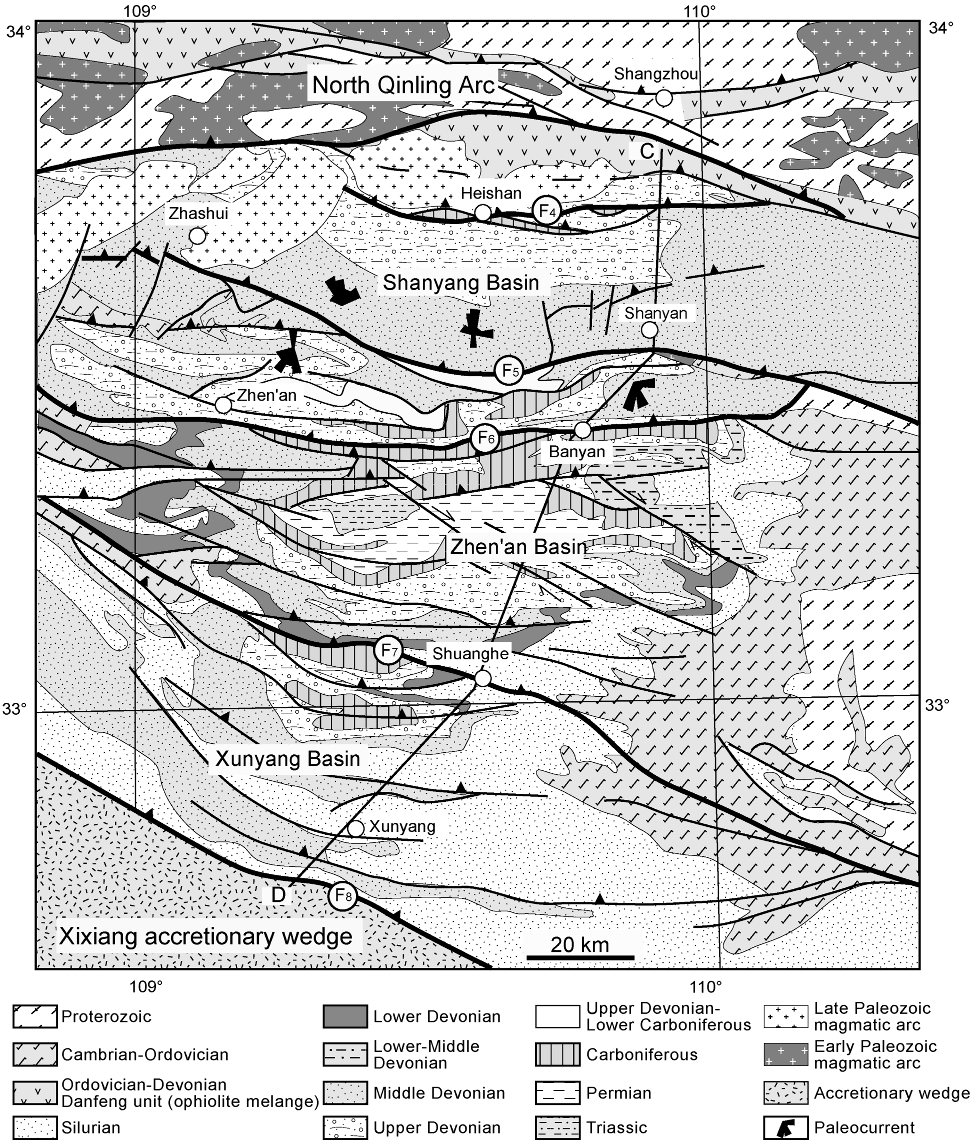

FIG. 5. Geological map of the Shanyang, Zhen'an, and Xunyang basins. Stratigraphic data from Li J. et al. (1994), Du D. (1986), and Zhang E. et al. (1993); palaeocurrent data from Meng et al. (1995); Symbols: F_4 = Heishan fault; F_5 = Shanyang fault; F_6 = Banyan fault; F_7 = Shuanghe fault; F_8 = Xunyang fault. Location of the structural section of Figure 6 is marked C–D.

typical textural and structural features of debris-flow alluvial fans (Nemec and Steel, 1984). Sandstones contain tabular and trough cross bedding (Fig. 7B). Massive sandstones occur both as tabular beds and as more lenticular bodies within stratified sandstones; they are fluvial channel sandstones (Miall, 1996). Abundant red mudstones and siltstones in the upper section were deposited on a floodplain. Variable fissility in thin beds, and blocky fracture in homogeneous beds are conspicuous. Grey massive siltstones contain abundant plant debris. Mud cracks and rain pits in fine-grained facies suggest that they were submerged during floods.

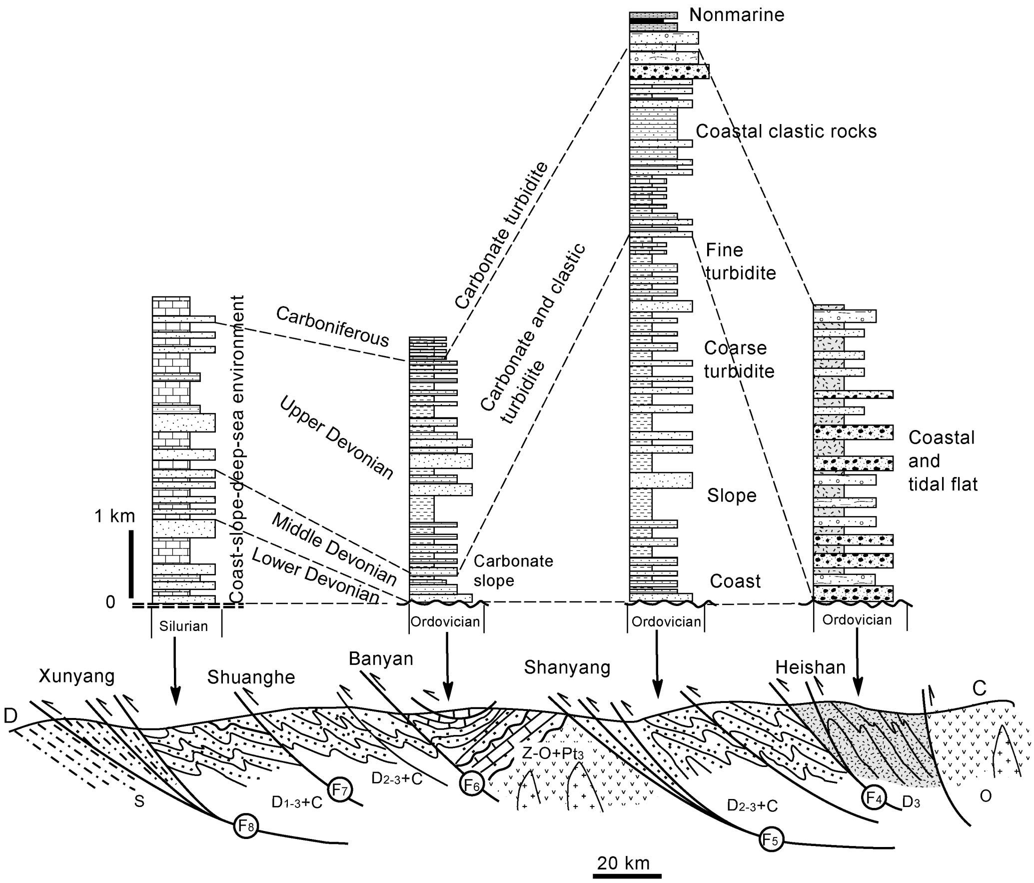

FIG. 6. Structural cross-section and sedimentary columns of the Shanyang, Zhen'an, and Xunyang basins (modified after Li J. et al., 1994). Symbols: $D_{1\text{-}3}$ + C = Lower-Upper Devonian and Carboniferous; $D_{2\text{-}3}$ + C = Middle–Upper Devonian and Carboniferous; D_3 = Upper Devonian; S = Silurian; Z-O = Sinian–Ordovician; Pz1 = early Paleozoic; O = Ordovician.

The Shujiaba Group is well exposed in the middle of the Xicheng basin (Fig. 3). It consists of coarse sandstone, siltstone, and mudstone with limestone interlayers. Grey siltstone with abundant ripples and parallel lamination (Fig. 7C) alternates with mudstone; higher in the section, massive-fine marls are juxtaposed against them. These are typical structures and textures of coastal deposits. However, grey massive conglomerate, sandstone, and mudstone constitute abundant cycles in lower sections (Fig. 4). Each cycle begins abruptly with coarser sandstone and grades upward into siltstone and mudstone. Massive conglomerate beds show graded bedding and scour base. Coarse- to medium-grained sandstones with faint parallel laminations are laterally continuous. Mud chips occur along base scour surfaces and ripple and wavy laminae in siltstones. Uniform and regular alternating beds of mudstone and siltstone with parallel and ripple laminae are very common. Sole and wave marks on the siltstones are commonly well developed (Fig. 7D). Slump structures (Fig. 7E) are present in siltstone and mudstone and *Nereites* ichnofacies in muddy siltstones and mudstones. These characteristics are diagnostic of submarine fan deposits (Howell and Normark, 1982).

The Xihanshui Group (Figs. 3 and 4) consists of sandstone, mudstone, lenticular reef and limestone blocks with Early to Late Devonian conodonts. Abundant Middle Devonian coral, bivalve, and

TABLE 1. Devonian Petrographic Assemblages, Sedimentary Structures, and Interpretation of Sedimentary Environments of the Xicheng Basin

Stratigraphic units	Fossils assemblages	Lithology	Sedimentary structures	Environments
Dacaotan Group	*Leptophloeum rhombicum Dnwson*, *Placodermi*, *Cyrtospirifer*, *Enniskilenia* sp., *Zaphrenitites* sp., *Acritarchs*, *Palaeochoristites* sp., *Eochoristites* sp., *Retispora lepidophyta*(kedo)playford	Conglomerates, coaly mudstones, and sandstone in the lower part; grey, greyish green sandstone and mudstone in the middle part; upper part contains red-brown mudstone, siltstone, and gray siltstone.	Lower part: crude graded-bedding, planar bedding, imbricated clasts, erosional base; middle part: parallel and graded bedding, cross-bedding; upper part: mud cracks, rain pits.	Fluvial deposits. Lower unit is deposited in channel and sheet flood deposits; middle units deposited in channel and longitudinal bars; upper units consists of floodplain or lake deposits and littoral-neritic carbonate.
Shujiaba Group	*Atrypa bodini* Manany., *Alveoljtella* cf. *arbuscula* Grahdispora cornuta Tumulispora., Rarituberculota., Cyclostigna, Kiltokense Haugh	Greyish green sandstone, calcareous and muddy sandstone, mudstone, and tuffaceous mudstone-dominated, massive marls in the upper section.	Ripple and flaser laminations, graded and massive bedding, sole marks, rhythmic bedding, and slump folds	Coastal to hemipelagic deposits. Coastal deposits in the upper section; conglomerates, coarse sandstone, and slump deposits in interchannel and overbank areas of the submarine fan; thickening-upward siltstone and mudstone cycles in the outer fan fringe.
Xihanshui Group				
Tieshan Formation	*Yunnanellina* sp., *Palmatolepis subperlobata, P.* cf. *subperlobata*, *P. delicatula delicatula*, *P. cf. regularis*, *p. gracilis gracilis*, *Palmatolepis quadrantinodosa*	Massive sandstone, mudstone with lenticular bioherm.	Small-current ripples, wave ripples, graded bedding	Lenticular limestone and sandstone with ripples and alternating bedding possibly deposited in a tidal flat.
Yushuping Formation	*Palmatolepis subperlobata, P. provera, Cyrtospirifer sp., Sinodisphyllum litvinovitschae, Pseudomicroplasma fungi, Alveolites* sp., *Uncinulus parallepipedus, Indiostroma* sp.	Grey thin- to thick-bedded, fine- to coarse-grained sandstone, muddy and sandy conglomerates with matrix-supported and lenticular reefs, micrite and sandy limestone. Carbonates are blocks or slices within the clastic rocks.	Ripple marks, rhythm sequence, flaser and graded bedding.	Cyclic sandstone and siltstone with ripple marks and graded bedding probably deposited in a tidal flat or a subaqueous slope by turbidity current. Conglomerates and massive sandstones may be filled in a channel or submarine canyon by slumps and debris flows. Limestone and reef with abundant shallow water fossils possibly filled in the channel by slumps.
Leijiaba Formation	Apiculiretusispora plicata, Acantnotriletes, Favosites sp., *Acropirifer* sp., *S. obesus*	Grey, dark mudstone, siltstone; fault contact between limestone and other units.	Sole marks, horizontal and graded bedding in siltstone unit; mass slumping in the limestone unit.	Turbidity deposits. Limestone unit was wrapped into the turbidite by gravity, possibly during sedimentation.

TABLE 2. Devonian Lithology, Sedimentary Structures, and Interpretation of Sedimentary Environments of the Shanyang, Zhen'an,and Xunyang Basins

	Shanyang Basin				Zhen'an Basin				Xunyang Basin			
Age	Formation	Lithology	Sedimentary structures	Environment	Formation	Lithology	Sedimentary structures	Environment	Formation	Lithology	Sedimentary structures	Environment
D_3	Tongyusi	Sandstone, conglomerate, lenticular limestone	Ripple marks, graded and cross bedding, slump structure	Nonmarine to shallow-water environment	Jiuliping	Sandstone, siltstone, mudstone	Graded bedding, scour base, convolution structure, sole mark, parallel laminae	Deep-water basin	Nanyangshan	Sandy oölitic limestone, micrite		
	Xiadonggou	Mudstone, marl, and bioclastic wackestone, micrite	Parallel and wavy laminae	Coastal environment					Lengshuigou	Sandstone, marl, bioherm, dolomite	Trough, flaser, and lenticular bedding	Tidal flats, reef
									Luojiayu	Sandstone, limestone	Wavy laminae	Tidal flats
D_2	Qingshiya	Siltstone, mudstone, marl with gastropods	Flaser, lenticular, herringbone bedding, mud cracks	Tidal flats	Xinghongpu	Sandstone, mudstone, bioherm	Reef and tidal flats		Yangjialing	Sandstone, marl, bioherm	Herringbone, and trough cross-bedding	Tidal flats and reef
	Chigou	Sandstone, siltstone, mudstone	Wavy and parallel laminae, lenticular and flaser bedding	Shelf-margin and tidal flat environments	Gudaoling	Limestone, conglomerate, sandstone	Graded and cross bedding, wavy laminae	Tidal flats	Dafenggou	Siltstone, mudstone, limestone	Tabular, trough, and wavy bedding	Tidal flat, reef, slope and shelf edges
	Niuerchuan	Sandstone, siltstone, limestone							Shijiagou	Marl and siltstone	Wavy and parallel laminae	
D_1									Gongguan	Dolomite, sandy limestone, sandstone with Pelecypoda	Trough and tabular cross-bedding, mud cracks, lenticular bedding	Tidal flat deposits
									Xichahe	Conglomerate, sandstone, siltstone, limestone with Pelecypoda	Ripple marks, graded and cross bedding, scour base	Subaqueous fan deposits

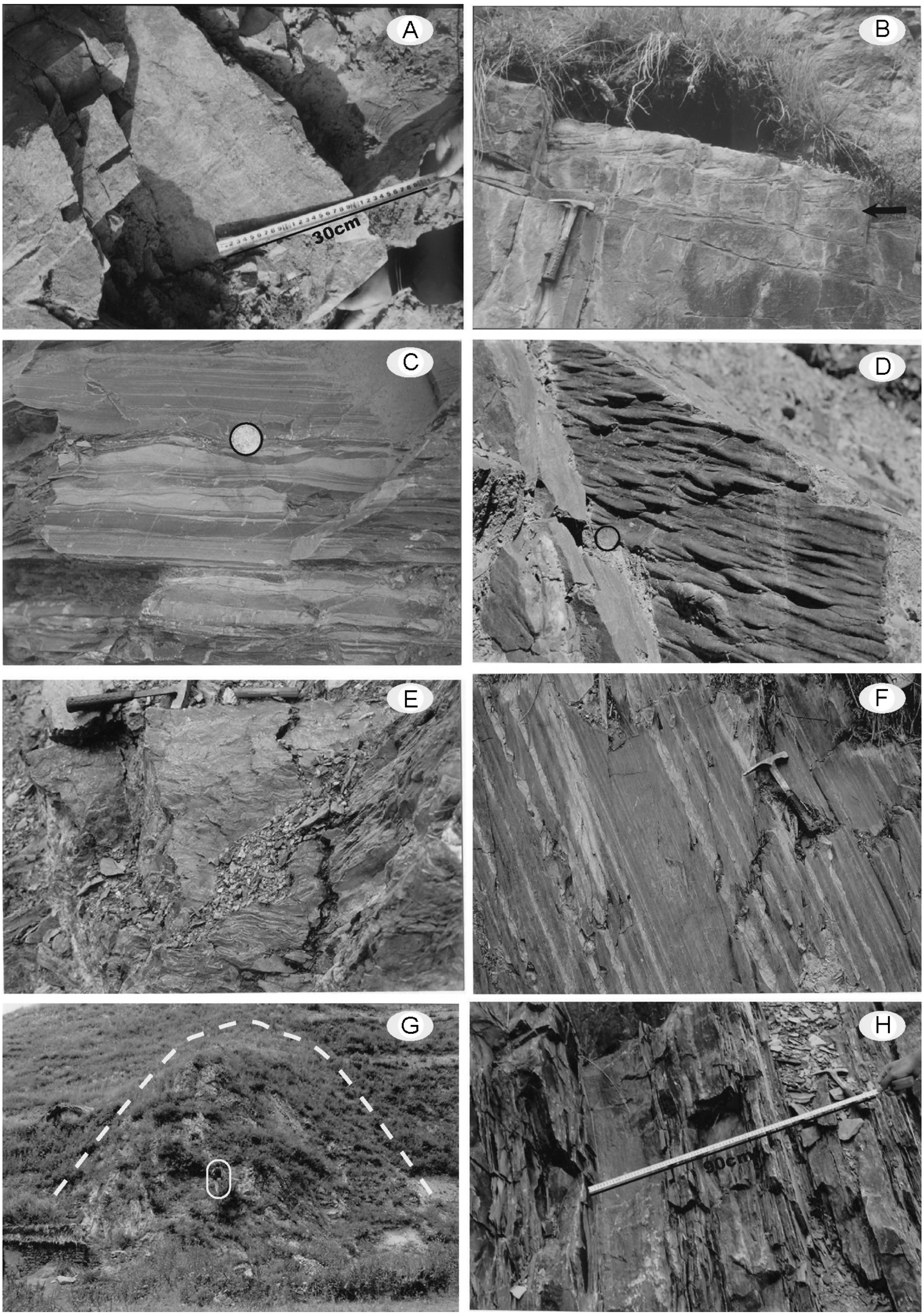

FIG. 7. Photographs of Devonian sediments in the Xicheng basin. A. Conglomerates with reverse grading and crude cross bedding (Dacaotan Group; ruler as scale indicating 30 cm). B. Sandstone with tabular cross bedding of the Dacaotan Group; paleocurrent from right to left. C. Turbidite of the Shujiaba Group, with scour base, ripple and parallel laminations; coin with 2 cm diameter in circle indicates scale. D. Sole marks on siltstone from the Shujiaba Group; coin with 2 cm diameter in circle indicates scale. E. Mudstone and siltstone slump of the Shujiaba Group. F. Turbidite consisting of mudstone (grey) and siltstone (darker grey) with ripple lamination from the Xihanshui Group. G. Reef block from the Xihanshui Group; person in circle indicates scale. H. Turbidite consisting of sandstone and mudstone from the Xihanshui Group; ruler as scale indicates 90 cm.

stromatopora fossils occur in the reef blocks. Thinner mudstone and siltstone are typical of the Leijiaba Formation lower in the section. Horizontal laminae, micro-graded bedding, sole marks, and abundant deep-sea trace fossils occur in siltstones. The Yushuping Formation, consisting of conglomerate, coarse sandstone, siltstone, and mudstone, stratigraphically overlies the Leijiaba Formation. Uniform, rhythmically bedded siltstone and mudstone are typical of this unit. Clear original bedding and lamination of clasts within matrix-supported synsedimentary conglomerates indicate slumping processes. Graded bedding is characteristic of sandstones. Erosion of sole marks occurs on the basal surfaces of sandstone, and siltstones with ripple laminae have good lateral continuity (Fig. 7F). These features are typical of sediments deposited by turbidity currents. Carbonate beds, including reef, micrite and sandy limestone, increase upward but are lenticular. Cyclic siltstones and mudstones with bioherms are well developed in the Wujiashan area. Flaser and ripple bedding in siltstones and mud cracks in mudstones are characteristic of tidal flat deposits. The Tieshan Formation overlying the Yushuping Formation consists of finer, thinner sandstones, mudstones with bioherms, and is characterized by regularly laminated, cyclic bedding in tuffaceous sandstones and mudstones (Fig. 7G). Each cycle begins with graded sandstone with an erosional base that grades upwards into siltstone with parallel lamination and ripple cross-bedding, and thinner mudstone (Fig. 7H). Lenticular bioherms developed around the Wujiashan fault migrate from southeast to northwest (Chen et al., 1992).

South of the basin, typical Devonian to Triassic flysch consists of sandstone and mudstone with chert and thinner limestone interbeds, indicating deep-water deposits. Sole marks are abundant and indicate that the detritus originated from the northeast (He, 1996).

Shanyang Basin

Deposits in the Shanyang Basin consist of: the Upper Devonian Tongyusi and Xiadongou formations; the Middle Devonian Niuerchuan, Chigou, and Qingshiya formations; and Carboniferous marine and nonmarine deposits (Fig. 6) that are separated by the Heishan fault (F4). The Tongyusi Formation is adjacent to the North Qinling arc and overlies the Danfeng unit unconformably (Fig. 5). In the Heihe area (Fig. 1), conglomerate, coarse sandstone, and siltstone, formed by gravity flows, built up several relatively small scale, fan deltas, slope aprons, and base-of-slope lobes, typically accompanied by slumps and slides along the Shangdan suture zone (Meng et al., 1994). The matrix of conglomerates is volcanic; clasts are complex, angular, and subrounded. Three different composite rock units occur in the Heishan area: (1) mudstone, limestone, and chert; (2) turbidite with pyroclastic rocks; and (3) conglomerate, sandstone, and siltstone. Ripple marks, grading, and cross-bedding are typical of the Tongyusi Formation (Figs. 8A–8C). Conglomerates are lenticular and matrix-supported with quick lateral changes. Angular sandstone and siltstone clasts show they were deposited near their source area, but were not transported for long distances. Grain size studies of sandstones indicate that the Tongyusi Formation was deposited in a shallow-water environment/continental slope (Zhou Z. et al., 1992).

The Niuerchuan Formation crops out in the east of the Shangyang area and consists of coarse sandstone, siltstone, and mudstone with graded bedding, scour base, and sole marks; mud cracks and ripple marks are developed in the mudstone and siltstone (Fig. 8D). Herringbone cross bedding and hummock bedding represent tidal flat deposits. Sandstone and siltstone are the main lithofacies of the Chigou Formation, with marl and mudstone in the upper part. Parallel lamination, ripple bedding, and smaller tabular cross bedding are characteristic of this unit. Sandy clastic rocks dominate in the lower section of the Qingshiya Formation, but mudstone and muddy siltstone occur mainly in the upper section; ripple lamination, crude graded bedding, and scour base are present in the sandstone. These characters suggest that the Qingshiya Formation is a coastal deposit. Parallel and ripple lamination in mudstone and thinner marl interbeds of the Xiadongou Formation were deposited on a tidal flat. Carboniferous clastic rocks, coal beds, and limestone interbeds with abundant plant fossils are tidal flat deposits.

Zhen'an Basin

Middle–Upper Devonian and Carboniferous sediments are the major infill of this basin. Conglomerate and coarse-graded sandstone occur dominantly in the lower part of the Lower Devonian Gudaoling Formation, and are succeeded by cyclic sandstone and limestone in the lower section of the formation; graded beds, scour base, and large, tabular, high-

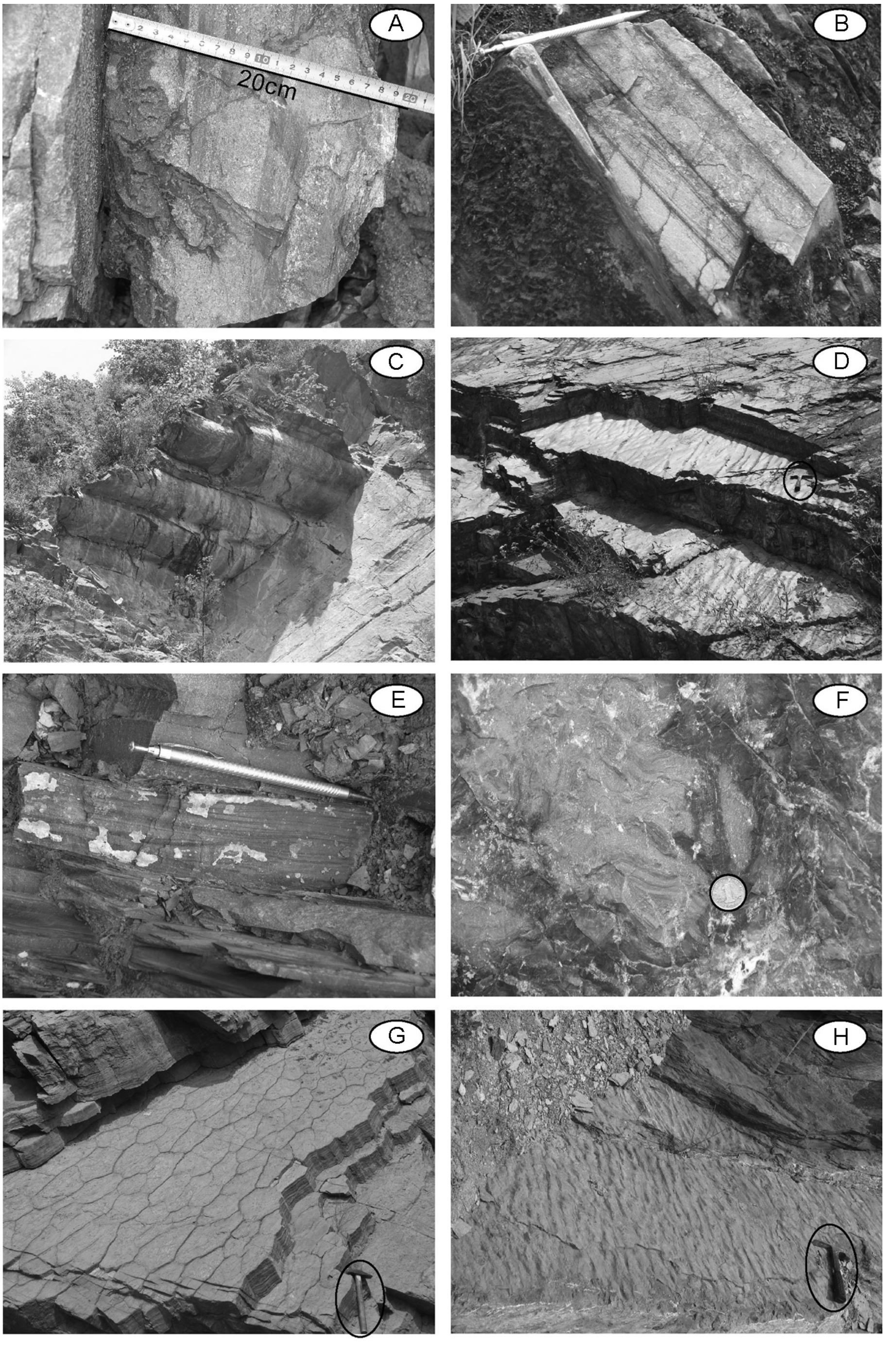

FIG. 8. Photographs of Devonian sediments in the eastern part of the Qinling. A. Conglomerates with graded bedding (Tongyusi Formation). B. Cross bedding in calcareous sandstone (Tongyusi Formation; pencil indicates scale). C. Large-scale symmetrical ripple marks of the Tongyusi Formation. D. Two different directions of wave-forming diamond diagrams in siltstone of the Niuerchuan Formation; the hammer in the circle indicates scale. E. Flaser bedding in mudstone (black) and siltstone (brown) of the Gudaoling Formation. F. Slump structures in the Gongguan Formation; coin with 2 cm diameter in circle indicates scale. G. Mud cracks in mudstone and siltstone of the Yangjialing Formation; hammer in circle indicates scale. H. Ripple marks in the Yangjialing Formation; hammer in circle indicates scale.

angle cross bedding reflect an alluvial apron environment. Flaser and lenticular bedding, ripple lamination, and parallel and cross bedding are typical in the upper section (Fig. 8E), indicating a tidal flat and carbonate platform. Conglomerate, coarse sandstone, siltstone, mudstone, and thinner marl beds of the Upper Devonian Jiuliping Formation have the clear texture and structure of turbidite. Graded bedding, scour base, sole mark, convolution structures, and parallel laminae are typical of this unit. Conglomerates with metamorphic and granite clasts are characteristic slump deposits (Meng et al., 1995). Carboniferous beds of thinner chert, limestone, and mudstone were deposited in a deep-water basin.

Xunyang Basin

Devonian deposits in the Xunyang Basin are complex but continuous. The Lower Devonian consists of the Xichahe and Gongguan formations. Dolomite, micrite, marl, and mudstone of the latter overlie the Xichahe Formation that consists of conglomerate, sandstone, and siltstone with scour base, cross beds, and current ripples. Slump structures occur in marls and mudstones (Fig. 8F). The conglomerate is matrix- and clast-supported, with graded bedding and scour base. Cyclic sandstone and conglomerate beds are prominent. Lithic fragments and clasts in the sandstone and conglomerate are angular, indicating a near-source deposit. Lenticular, wavy flaser bedding, trough and tabular cross bedding, small-scale ripple cross-bedding, and parallel bedding are prominent in the Gonguan Formation. These features suggest that Lower Devonian sedimentation took place in a tidal flat and shelf. Marl, muddy siltstone, and dolomite interbeds of the middle Devonian Shijiagou Formation are covered by cyclic carbonate and sandstone of the Dafengou Formation. The Luojiayu and Yangjialing formations are two units of the middle part of the Middle Devonian. Carbonates are developed in the lower part of the Luojiayu Formation. Well-sorted sandstone and micrite of the Yangjialing Formation overlie the Luojiayu Formation. Flaser, lenticular bedding, mud cracks (Fig. 8G), and wavy marks (Fig. 8H) suggest the Luojiayu and Yangjialing formations are tidal deposits. The Upper Devonian includes the Lengshuihe and Nanyangshan formations that consist of sandstone, marl, mudstone, bioclastic micrite, dolomite, and biolithite. Large-scale, compound cross bedding, parallel lamination, lenticular and flaser bedding, and ripple cross-bedding suggest they were deposited in shelf-margin and peritidal environments. Lenticular, flaser ripple bedding, mud cracks, and tabular and trough cross bedding are typical structures of the Nanyangshan Formation, indicating a tidal flat environment.

Sandstone Provenance and Tectonic Setting

Paleocurrent indicators

Abundant, diverse paleocurrent and paleoslope indicators, including syndepositional slump folds, cross bedding and ripple stratification, imbricate gravels, and sole marks, occur in the Devonian basins. The paleocurrent indicators in the Xicheng Basin have two directions (Fig. 3). Cross bedding, sole marks, and imbricated clasts of the Dacaotan and Shujiaba groups point to a uniform southward trend, suggesting that their source area is located in the northern margin of the basin. However, studies on the paleocurrent indictors from the Xihanshui Group indicate a northward direction. In the Wujiashan-Xihe areas, paleocurrent directions are complex and indicate the presence of an old uplift that provided detritus for the basin.

In the Shangyang Basin, cross bedding and imbricated clasts of the Tongyusi Formation suggest their source area was located to the north (Zhou Z. et al., 1992); heavy mineral assemblages also support this derivation. Clasts of the conglomerates in the Xunyang Basin have Silurian, Proterozoic, and Cambrian–Ordovician ages (Yin and Huang, 1995). The northwest paleocurrent indicators of sediments in the Xunyang Basin suggest derivation from the southeast. These relations demonstrate that old metamorphic blocks of the basement, today occurring in the southeast margin of the basin, were an important source of basinal sediments (Fig. 5).

On the other hand, Devonian paleocurrent indicators on both sides of the Shangyang fault have contrary directions (Fig. 5; Meng et al., 1995). Metasandstone, granitic and metamorphic clasts of the Jiuliping Formation indicate derivation from an old basement. Conglomerates adjacent to the Shangyang fault only occur on the northern margin of the Zhen'an Basin. This indicates that their source area was located in the northern margin of the basin, which is consistent with the paleocurrent indicators.

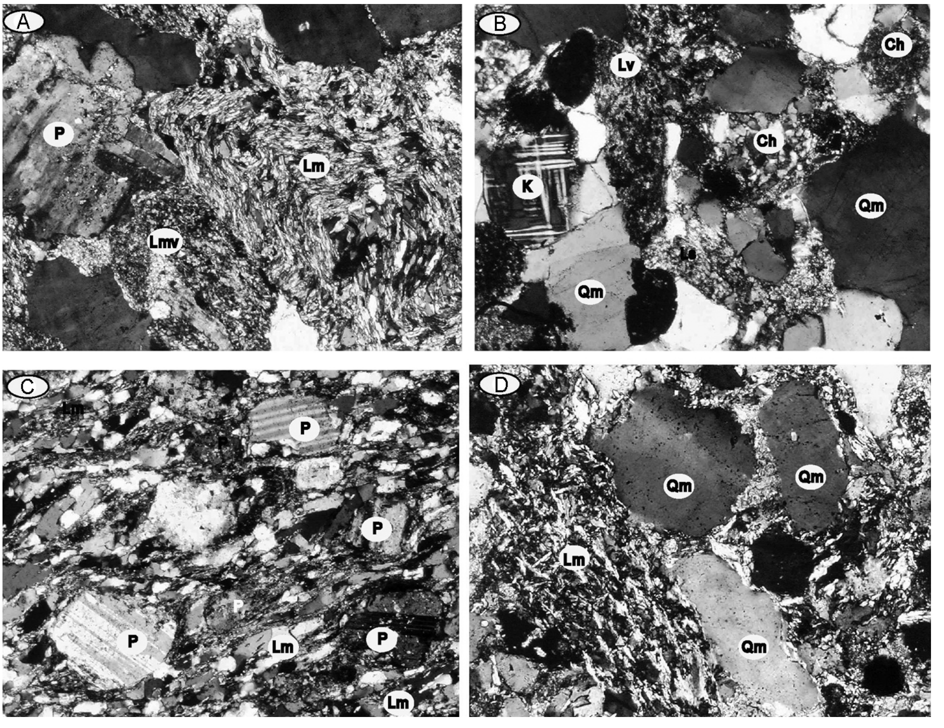

FIG. 9. Textures of graywacke and arkose of the Devonian System from the Xicheng Basin. A. Plagioclase (P), schist (Lm), and metavolcanic (Lmv) fragments of graywacke from the Dacaotan Group (sample of B020; field of view 3.1 mm). B. Granite with microcline (tartan twinned; K) and quartz (untwined; Qm), aphanitic volcanic (Lv), and chert (Ch) fragments of graywacke from the Dacaotan Group (sample of B1074; field of view 3.1 mm). C. Deformed arkose with abundant angular plagioclase (P; parallel twining) from the Shujianba Group (sample of B095; field of view 3.1 mm). D. Graywacke from the Xihanshui Group containing a mica-quartz schist fragment with a foliated texture (Lm), and abundant inclusions in the quartz fragments (Qm), indicating granite origin (sample of B1020; field of view 1.7 mm).

Detrital modes

Sedimentation of the conglomerate and associated turbidite and pyroclastic rocks in the Dacaotan Group and the Tongyusi Formation was evidently related to development of the North Qinling rather than the South Qinling. The Tongyusi Formation—with its many small-scale fan deltas, slope aprons, base-of-slope lobes, slumps, and slides along the Shangdan suture zone—reflects a linear-source sediment supply, and is characteristic of active continental margins (Chan and Dott, 1983; Heller and Dickinson, 1985). The spatial variations of conglomerate compositions result from diversity of provenances in different areas, but the common association with volcanic-clastic rocks in almost all conglomeratic bodies indicates that the generation of conglomerate probably was coeval with nearby volcanic activity. Gravels in the conglomerates were derived from the Qinling unit and ophiolitic rocks with island-arc features (Zhang B. et al., 1994; Zhang C. et al., 1997). Geochemical and petrological analyses also show that turbiditic sandstone and pyroclasts formed in an active continental margin or continental island arc (Yu et al., 1991). Conglomerates of the Xichahe Formation in the Xunyang Basin with their abundant angular Silurian chert and mudstone clasts show that the Silurian basement provided sediments for the basin. Heavy mineral assemblages of the sandstone demonstrate that the North Qinling provided abundant sediments for the Devonian marine deposits (Zhou Z. et al., 1992).

Coarse-grained clastic units in the Devonian basin are chiefly feldspathic sandstone and lithic greywacke (Fig. 9). Using the Gazzi-Dickinson petrographic approach (Ingersoll et al., 1984), we studied the framework-grain compositions of sandstone samples from the Xicheng Basin. Unfortunately, altered samples of the Shujiaba and Xihanhui groups were difficult to point count using 350 framework-grain points per slide. The total points (69 to 506; see Appendix 1) are a reflection of the grain size, composition, and the grain density/distribution across the thin sections. Raw point-count data and recalculated parameters of 48 samples for the sites are listed in Appendices 1–3. These samples are typified by a somewhat greater abundance of lithic fragments (average 50%) than quartz (average 24%) and feldspar (average 26%). Volcanic, plutonic, and metamorphic fragments are major lithic grains of the Dacaotan Group (Figs. 9A and 9B), but the content of volcanic and plutonic fragments decreases and nonvolcanic lithic proportions increase distinctly in the thin-sections of the Shujiaba and Xihanshui Groups (Figs. 9C and 9D). The proportion of plagioclase feldspar fragments is higher (e.g., B092: 52%) in samples of the Shujiaba Group (except for B093) and the Xihanshui Group than in the Dacaotan Group (see Appendix 2). The mica content was similar (up to 8% of framework grains) in some thin sections of the Shujiaba and Xihanshui groups. Commonly, quartz fragments are monocrystalline and polycrystalline with evident scaly inclusions (Fig. 9D) and undulatory extinction, which means those quartz fragments originated from an old metamorphic region. Monocrystalline quartz (inclusionless, and with uniform extinction) and potassium feldspar in the samples suggests at least a partial felsitic volcanic or shallow-intrusive source (Fig. 9B).

In order to study the evolution of tectonic provenance, we used the mean of sandstone compositions rather than individual data points to produce an actualistic provenance model of the Devonian sandstones of the Xicheng Basin (see Appendix 3). Sandstone samples fall in the transitional-arc field of Dickinson (1985), and indicate that they have an island-arc setting (Fig. 10A). The proportion of feldspar fragments of the Shujiaba Group and the Xihanshui Group increases southward in the basin (Figs. 3 and 10A), but there is no distinctive variation in the detrital composition of the Dacaotan Group. On a QmKP triangular plot (Fig. 10B), sandstone samples with higher quartz contents (QmPKQm% varies from 27 to 60) have the characteristics of triple-junction and continental-arc sandstones (Marsaglia and Ingersoll, 1992). The compositions of modern sediments from different known tectonic settings demonstrate that sandstones in triple-junction and strike-slip continental-arc sites are variable in composition, but in intra-oceanic and remnant arcs they are consistently dominated by volcanic lithics, and in continental arcs show only slightly higher percentages of metamorphic and sedimentary lithic fragments (Marsaglia and Ingersoll, 1992). However, the Devonian sandstone samples of the Xicheng Basin have an overall dominance of a metamorphic lithic component of 37 to 78% (Fig. 10C), which indicates that the Devonian sandstones are related to a continental arc.

Marsaglia (1991) discussed the importance of microcrystalline volcanic lithic textures in greywackes. Microcrystalline volcanic lithic proportions for arc-related sandstones indicate an overall dominance of microlitic textures and a maximum felsitic component of 40%. Continental arcs show a wide range of values, but strike-slip continental-arc sandstones have felsitic percentages greater than 5% and triple-junction sandstones are bimodal (Marsaglia and Ingersoll, 1992). The felsitic component of the Devonian sandstone is variable (from 8.0 to 23%), except for one site (Shixia). All the Devonian samples with a high content of microlitic (andesitic) fragments indicate that they originated from a continental-arc setting. Samples from the Shixia area fall in the microlitic pole of an LvfLvmiLvl plot (Fig. 10D), which belongs to the intra-oceanic arc field of Marsaglia (1991).

Major and trace elements of Devonian siltstone

Sediments in different tectonic settings have distinctive geochemical characteristics. Bhatia (1983) and Bhatia and Crook (1986) suggested a simplified plate-tectonic classification of continental margin and oceanic basins based on the nature of the crust from which the sediments were derived. The geochemical signatures of the Devonian siltstone and mudstone (Appendix 4) clearly suggest derivation from an arc, either continental or oceanic (Figs. 11A and 11B). Using the Bhatia (1983) discriminant functions for the major-element contents of the Devonian siltstone and mudstone supports the idea that the sediments were sourced completely from an active continental margin (Fig. 11C).

Trace-element (e.g., Th and Sc) and rare-earth-element (REE) distributions in sedimentary rocks provide reliable provenance indictors because they tend to be transferred unfractionated into sediment and therefore reflect the average REE composition

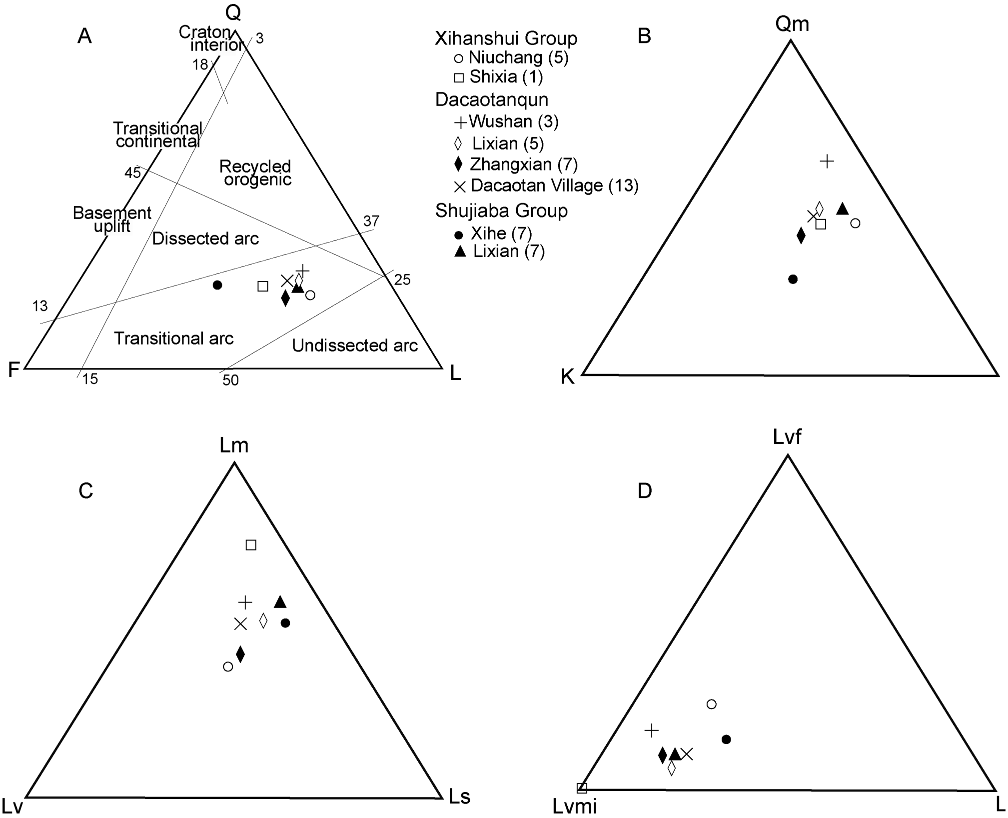

FIG. 10. Ternary plots of relative proportions of framework-grain compositions for Devonian graywacke and arkose from the Xicheng basin. Symbols: Q = total monocrystalline (Qm) and polycrystalline (Qp) quartz grains; F = total potassium feldspar (K) and plagioclase (P) grains; L = aphanitic unstable lithic grains, including sedimentary (Ls), metamorphic (Lm) and volcanic (Lv) fragments; Lvf = felsitic fragments; Lvmi = microlitic (andesitic) fragments; Lvl = lathlike (basaltic) fragments. The dot in the plot represents mean value; number in the bracket represents total samples.

of the source (McLennan et al., 1990). On La-Th-Sc, Th-Sc-Zr/10, and La-Th discriminator plots (Figs. 11D–11F), Devonian siltstone and mudstone fall in the continental-arc field. Chondrite-normalized REE distribution patterns for Devonian siltstone and mudstone (Fig. 12) typically show light REE enrichment, relatively flat heavy REE trends, and Eu anomalies ranging from Eu/Eu* = 0.4–0.78. These are consistent with typical REE patterns for modern deep-sea turbidites from a continental island arc tectonic setting (McLennan et al., 1990), and variable Th/Sc and La/Sc ratios and negative Eu anomalies are consistent with derivation from young differentiated arcs.

Song H. et al. (1995), Yu and Meng (1997), and Yu et al. (1991) studied the metamorphic greywacke in the Shanyan Basin and proposed a forearc setting using geochemical analysis. Devonian mudstone and greywacke samples from the Shanyang, Zhen'an, and Xunyang basins exhibit low, quite restricted ranges of La/Th (1.0–3.5) and Sc/Th (0.6–1.5), and form sublinear arrays that are centered on the North Qinling and away from the upper crustal compositions of the SCB (Gao et al., 1995). Some samples with high Th/Co > 1.0 and Sc/Th are similar to those of North Qinling and SCB sediments. This may suggest a greater contribution from the SCB. However, their highly consistent similarity in chemical compositions with those of the North Qinling and the scarcity of samples with La/Th > 3.5 make it unlikely that this area played an important role for all the Devonian basins. A significant contribution from the South Qinling basement is also not supported by the very high La/Co ratios of the South

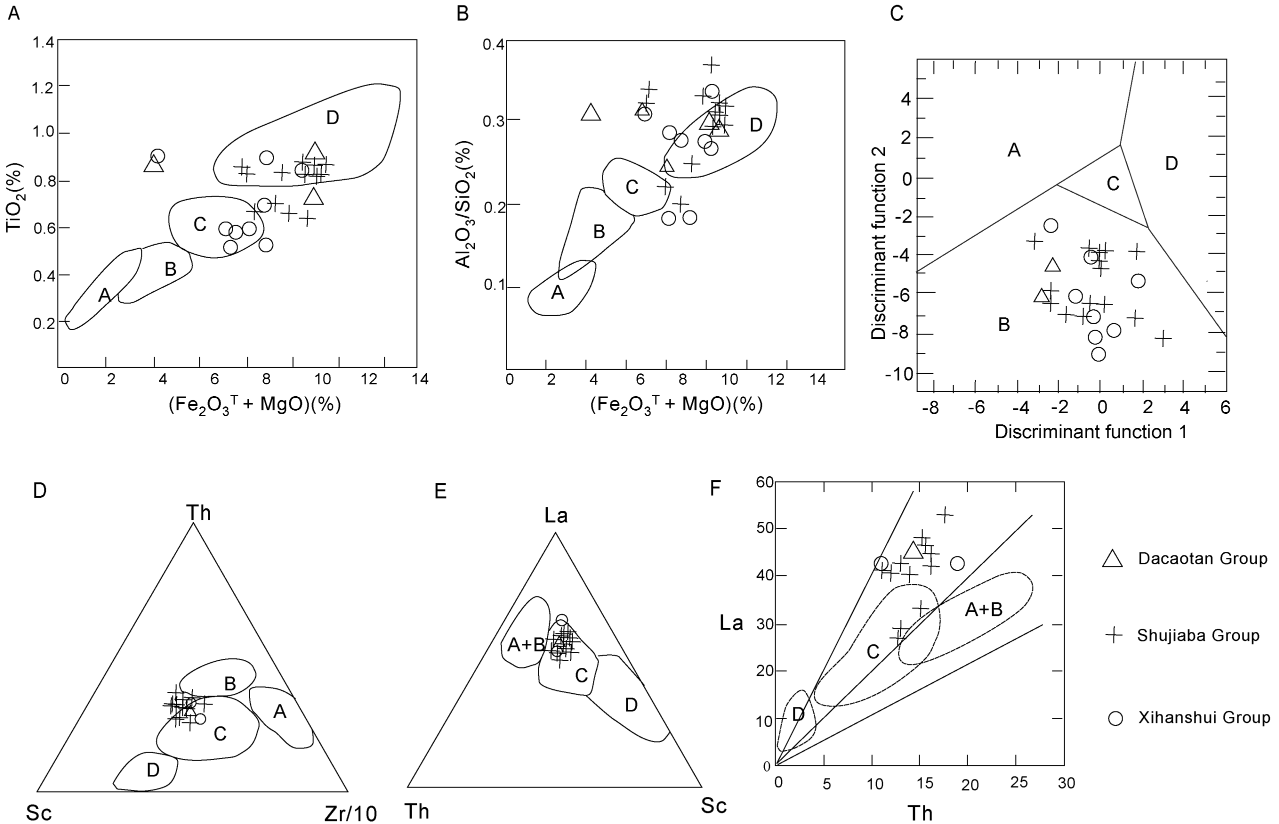

FIG. 11. Discriminant plots of major and trace elements from Devonian siltstones and mudstones of the Xicheng basin. Outlined fields: passive margin (A); active continental margin (B); continental island arc (C); oceanic island arc (D) (Bhatia, 1983; Bhatia and Crook, 1986). Discriminant function 1 = –0.0447 SiO_2 – 0.972 TiO_2 + 0.008 Al_2O_3 – 0.267 Fe_2O_3 + 0.208 FeO – 3.082 MnO + 0.140 MgO + 0.195 CaO + 0.719 Na_2O – 0.032 K_2O + 7.510 P_2O_5 + 0.303; Discriminant function 2 = –0.421 SiO_2 + 1.988 TiO_2 –0.526 Al_2O_3 – 0.551 Fe_2O_3 – 1.610 FeO – 2.720 MnO + 0.881 MgO – 0.907 CaO – 0.177 Na_2O – 1.840 K_2O + 7.244 P_2O_5 + 43.57.

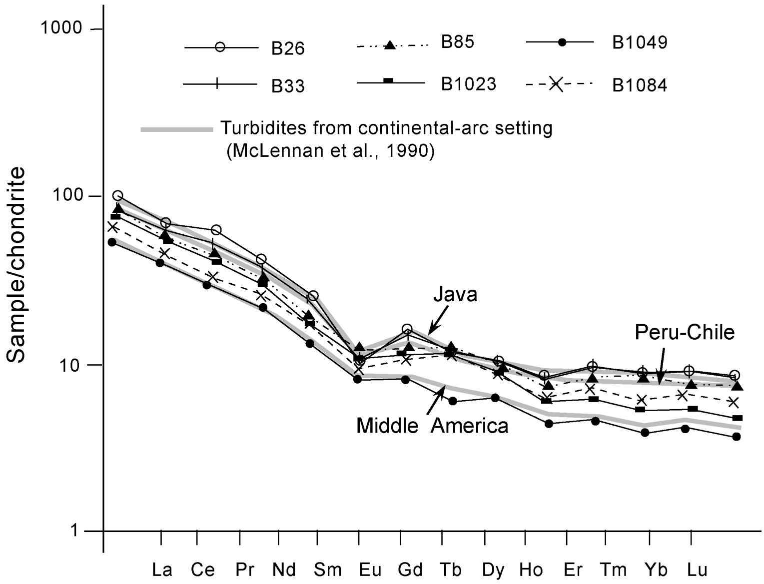

FIG. 12. Chondrite-normalized REE distribution patterns for Devonian siltstone and mudstone from the Xicheng Basin. Grey lines for sands from Mid-America, Peru-Chile, and Java (McLennan et al., 1990).

Qinling sediments. On the other hand, Liu et al. (1989) suggested that the clastic provenance of the Devonian South Qinling basins was principally from North Qinling, which needs future study.

Discussion

Tectonic settings and sedimentary environments of Devonian basins

The tectonic setting of the South Qinling Devonian basins has been a prolonged question in studies of the Qinling orogen. They have been interpreted as pull-apart basins (Huo and Li, 1995; Fang et al., 2001), foreland basins (Mattauer et al., 1985; Cao et al., 1990; Li J. et al., 1994; Du Y., 1997), forearc basins (Li C. et al., 1978; Yang, 1999; Wang Z. Q. et al., 2002; Yan, 2002), or accretionary wedges (Ratschbacher et al., 2003). These different views seriously hamper studies of the Paleozoic evolution of the Qinling orogen within the tectonic framework of East Asia.

Regionally, the North Qinling comprises ~470–490 Ma oceanic island arcs (Danfeng arc) and ~400 Ma accretionary magmatic arcs. A complex and prolonged accretionary wedge formed from the Silurian (?) to the Early Triassic, due to north-dipping subduction of an ocean basin north of the SCB. During subduction and accretion, Devonian sedimentation took place between these units. Subduction resulted in the uplift and erosion of arc terrains and accretionary wedges to produce abundant sediments for the forearc region.

Geochemical and petrological analyses of conglomerates and associated turbidites and pyroclastic rocks, combined with paleocurrent indictors demonstrate that these sediments were deposited in forearc regions and that development was evidently related to that of the North Qinling arc. The abundant detritus of the Devonian deposits was also derived from the Qinling unit and ophiolitic rocks with an island-arc association, suggesting that an accretionary wedge was also a source of the Devonian sediments. Paleocurrent indictors within the basins indicate that some basement uplifts were eroded and truncated to produce small-scale, coarse-grained, slope aprons or base-of-slope lobes around faults.

The sedimentary environments of the Devonian basins are typically asymmetric, with the deepest water at or near the bounding accretionary wedge (Figs. 4 and 6). Where uplift of the trench-slope break was sufficient, ponding of sediment during underfilled phases of basin evolution produced basin-plain turbidite environments of limited areal extent along the keel of a deep forearc trough. Lateral progradation of depositional systems caused shelf-slope assemblages related to the arcward flank of the basin. Fan channel fills composed of detritus derived from the arc terrains are prominent along the arcward flanks of basins. Shelf assemblages include prominent carbonate reefs and buildups with associated slope aprons of carbonate turbidite deposits, and basinal deep-water successions include finer turbidite deposits. The depocenters and associated facies belts migrated arcward into the basins (Figs. 4 and 6) during Devonian forearc sedimentation. Consequently, a shallow-marine and turbidite depositional system evolved into complex patterns to produce a varied facies framework in both time and space. On the other hand, transpressional and transtensional effects related to slip on forearc strike-slip faults influenced the tectonic evolution of the sub-basins. Such a relationship was recorded by locally derived turbiditic fan complexes in these half-graben sub-basins shed from intrabasinal fault blocks oriented transverse to the trend of the arc-trench system. These characteristics of the late Paleozoic sedimentary basins in the South Qinling are very similar to the facies framework of the Sunda forearc basins (Beaudry and Morrem, 1981; Matson and Moore, 1992).

Evolution of the Paleozoic sedimentary basins

Arcs and forearc basins are two paramount units of collisional orogenic belts. Although they are often strongly deformed, metamorphosed, and fragmented by post-accretion tectonic activity, the structural architecture and the presence of the syntectonic sediments in forearc basins provide key insights to the evolution of forearc region in collisional mountains and help to identify the orogenic framework (Puchkov, 1997; Brown and Spadea, 1999; Xiao W. J. et al., 2002a; 2002b; 2003). The Qinling is an accretionary orogen that developed into a collisional orogen. It preserves a record of late mid-Proterozoic to Cenozoic tectonism in central China. Ratschbacher et al. (2003), Meng and Zhang (1999), Gao et al. (1995), Lerch et al. (1995), and Li C. et al. (1978) defined this process from the Early Ordovician to the Late Triassic. A thick Devonian sequence (up to 4000 m) in the forearc basins records the accretion along the North Qinling arc.

In Early to Middle Ordovician time, an oceanic island arc developed south of the NCB. A trondhjemitic dike with a $^{207}Pb/^{206}Pb$ single zircon age of 488 ± 8 Ma (Reischmann et al., 1990), which intruded volcano-sedimentary lithologies with island arc affinities in the Danfeng area (Xue et al., 1996b), defines a minimum age for the Danfeng island arc, which collided later with the NCB. Detritus from the island arc was deposited in the forearc region. A north-dipping subduction zone was initiated following accretion of the island arc, resulting in calc-alkaline magmatism from the Late Silurian to the Early Devonian (Fig. 13A). In the Middle Devonian, the north-dipping subduction resulted in uplift of the early deposits in the forearc basin and in southward accretion (seaward). Progressive overlap and mass slumping were initiated after subduction and accretion (Fig. 13B). The forearc basin was broken into sub-basins by thrust faults. A thrust sheet and one part of the accretionary wedge were marginal to these sub-basins and provided detritus for them. Tidal flat, slope, and shelf deposits developed around the thrust-ramp. During the Late Devonian, calc-alkaline magmatism migrated southward and intruded the early deposits, and provided pyroclastic sediments for deposition (Fig. 13C). The accretionary wedge also increased in volume and ponded the sediments. Nonmarine sediments developed adjacent to the island arc and a shallow-marine environment was preserved around the thrust sheet.

In the Carboniferous to Permian, northward subduction made the forearc basin and North Qinling arc uplift, and gave rise to nonmarine sedimentation (Fig. 13D). Marine deposition dominantly took place in the northern part of the SCB. In the NCB, Middle Carboniferous to Lower Permian coal-bearing series were deposited and andesitic volcanic rocks were generated (Zhang H. et al., 1997). In the northern margin of the SCB, Carboniferous–Permian deposits were also added to the accretionary wedge (Ratschbacher et al., 2003). In the Early to Middle Triassic, subduction of the Qinling ocean resulted in development of island-arc calc-alkaline volcanic rocks along the southern margin of the NCB (Lai and Zhang, 1996). The leading edge of the SCB was subducted to >150 km below this orogen and to the depth greater than 200 km below the Dabie orogen to the east (Ye et al., 2000). They were subsequently exhumed by crustal extension during clockwise rotation of the plate (Ratschbacher et al., 2003). Abundant plutons intruded the basin and initiated development of a ca. 400 km long granitiod belt in the South Qinling. In the Late Triassic, collision between the NCB and SCB resulted in extensive syncollisional granitoids ranging from I-type to S-type in the South Qinling (Li S. et al., 1993). The ocean died, and an ocean basin with a thick flysch sequence was transformed into a relict basin with

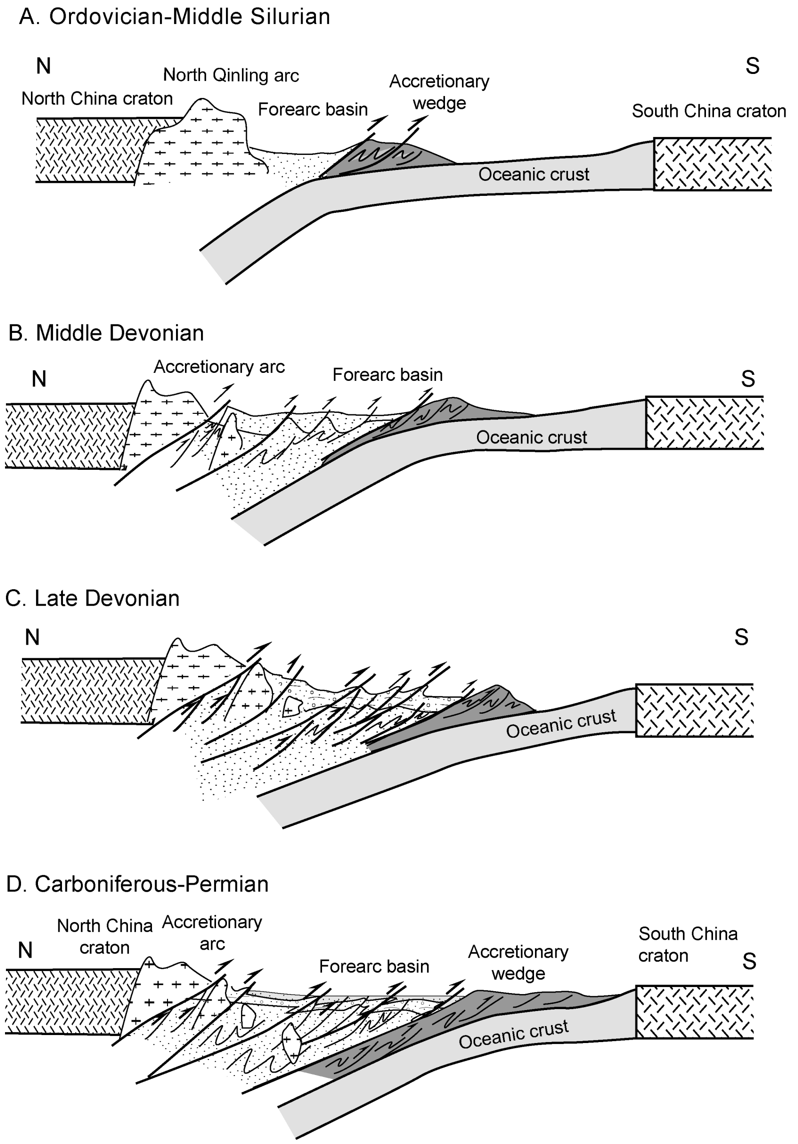

FIG. 13. Sequential diagram showing the evolution of the late Paleozoic forearc basin in the Qinling orogen. A. Late Silurian to Early Devonian. B. Middle Devonian. C. Late Devonian. D. Carboniferous to Permian. See text for discussion.

nonmarine deposits. This development might be attributed to intracontinental collision and crustal thickening due to strong northward movement of the SCB in the Late Triassic.

Subduction of the oceanic crust was probably oblique, resulting in concurrent strike-slip faulting. In this scenario, part of the arc including the accretionary wedge would have been removed by strike-slip faulting, and the forearc basins were broken into sub-basins with a thrust-based basin margin.

Acknowledgments

YZ thanks Prof. C. F. Jiang, who exercised a decisive influence on his professional development and rendered him enormous help in his studies of the Qinling orogen. Brian Windley kindly read the manuscript, and all the corrections are appreciated. Funding by the Chinese Academy of Sciences (KZCX2-SW-119-01), and the Projects of the Geological Surveying Project of China (DKD2001002) and the Chinese National Science Foundation (40334044) is gratefully acknowledged.

REFERENCES

Ames, L. G., Tilton, G. R., and Zhou, G., 1993, Timing of the Sino-Korea and Yangtze cratons: U-Pb zircon dating of coesite-bearing eclogites: Geology, v. 21, p. 339–342.

BGM Gansu (The 7th Geological Team of the Bureau of Geology and Mineral Resources of Gansu Province), 1982, Geological and mineral mapping and report of Tianshui area, 1:200,000 (in Chinese).

BGM Shaanxi (Geological Survey Team of the Bureau of Geology and Mineral Resources of Shannxi Province), 1999, Geological Map of the Liuba area (I-48-E015020), 1:50,000 (in Chinese).

BGM Shaanxi (Geological Survey Team of the Bureau of Geology and Mineral Resources of Shannxi Province), 1994, Geological Maps of the Yaoping (I-48-92-D), Baishuijiang (I-48-93-A), Shangliangheko u (I-48-93-B), Xujiaping (I-48-93-C), and Lianghekou (I-48-93-D) areas, 1:50000 (in Chinese).

Beaudry, D., and Morrem G. F., 1981, Seismic-stratigraphic framework of a forearc basin off central Sumatra, Sunda arc: Earth and Planetary Science Letters, v. 54, p. 17–28.

Bhatia, M. R., 1983, Plate tectonics and geochemical composition of sandstones: Journal of Geology, v. 91, p. 611–627.

Bhatia, M. R., and Crook, K. A. W., 1986, Trace element characteristics of greywackes and tectonic setting discrimination of sedimentary basins: Contributions to Mineralogy and Petrology, v. 92, p. 181–193.

Brown, D., and Spadea, P., 1999, Processes of fore-arc and accretionary complex formation during arc-continent collision in the southern Ural Mountains: Geology, v. 27, p. 649–652.

Cao, X., Zhang, R., and Zhang, H., 1990, On stratigraphy and sedimentary environment of important ore-bearing horizon in Devonian Period, Qinling-Dabashan area, China: Bulletin of Xi'an Institute of Geological Mineral Resources, Chinese Academy of Geological Sciences, v. 23, p. 1–124 (in Chinese).

Chan, M. A., and Dott, R. H., Jr., 1983, Shelf and deep-sea sedimentation in an Eocene forearc basin, western Oregon-Fan or non-fan?: American Association of Petroleum Geologists Bulletin, v. 67, p. 2100–2116.

Chen, B., Xin, J., and Xin, W., 1992, Continental slope-submarine canyon-submarine fan system of Shujiaba Group, northern belt of Western Qinling, *in* Liu, B., Xiao, J., and Zhou, Z., eds., A selection of papers on the sedimentary geology of the paleo-continental passive margin: Wuhan, China, China University of Geosciences Press, p. 25–36 (in Chinese with English abstract).

Cui, Z., Sun, Y., and Wang, X., 1996, A discovery of radiolaria from the Danfeng ophiolites, North Qinling and its tectonic significance: Chinese Science Bulletin, v. 41, no.11, p. 916–919.

Dickinson, W. R., 1985, Interpreting provenance relations from detrital modes of sandstones, *in* Zuffa, G. G., ed., Provenance of arenites: Dordrecht, The Netherlands, Reidel Publishing Company, p. 333–362.

Du, D., 1986, Study of the Devonian of the Qinba area, Shaanxi province: Xi'an, China, Xi'an Jiaotong University Press, 230 p. (in Chinese with English abstract).

Du, Y., 1997, Devonian sedimentary geology of Qinling orogenic belt: Wuhan, China, China University of Geosciences Press, 130 p. (in Chinese with English abstract).

Duanmu, H., 2000, The conglomerates controlled by synsedimentary faults of the Devonian in Fengxian-Shanyang, Shaanxi province: Journal of Palaeogeography, v. 2, p. 92–98 (in Chinese with English abstract).

Fang, W., Zhang, G., and Li, Y., 2001, Characteristics and implications of extensional tectonics in the Upper Palaeozoic in the Qinling orogenic belts: Journal of Northwest University, v. 31, p. 235–240.

Feng. Q., Du, Y., Yin, H., and Sheng, J., 1996, Carboniferous radiolaria fauna first discovered in Mianlue ophiolitic mélange belt of South Qinling Mountains: Science in China, v. D39 (suppl.), p. 87–92.

Gao, S., Zhang, B.-R., Gu, X.-M., Xie, Q.-L., Gao, C.-L., and Guo, X.-M., 1995, Silurian–Devonian provenance changes of South Qinling basins: Implications for accretion of the Yangtze (South China) to the North China cratons: Tectonophysics, v. 250, p. 183–197.

Hacker, B. R., Ratschbacher, L., Webb, L., Ireland, R., Walker, D., and Dong, S., 1998, U/Pb zircon ages constrain the architecture of the ultrahigh-pressure Qinling-Dabie Orogen, China: Earth and Planetary Science Letters, v. 161, p. 215–230.

He, H., 1996, Early Triassic sediments and their controlled factors, western Qinling: Acta Sedimentologica Sinica, v. 14, no.1, p. 86–92 (in Chinese with English abstract).

Heller, P. L., and Dickinson, W. R., 1985, Submarine ramp facies model for delta-fed, sand-rich turbidite systems: America Association of Petroleum Geologists Bulletin, v. 69, p. 960–976.

Howell, D. G. and Normark, W. R., 1982, Submarine fans, *in* Scholle, P. A., and Spearing, D. R., eds., Sandstone depositional environments: Tulsa, OK, American Association of Petroleum Geologists, p. 365–404.

Hu, N., Yang, J., An, S., and Hu, J., 1993, Metamorphism and tectonic evolution of the Shangdan fault zone, Shaanxi, China: Journal of Metamorphic Geology, v.11, p. 537–548.

Huang, W., and Wu, Z., 1992, Evolution of the Qinling orogenic belt: Tectonics, v. 11, p. 371–380.

Huo, F., and Li, Y., 1995, Evolution of the Western Qinling orogenic belt: Acta Geological Gansu, v. 5, p. 1–15 (in Chinese with English abstract).

Ingersoll, R. V., Bullrad, T. F., Ford, R. L., Grimm, J. P., Pickle, J. D., and Sares, S. W., 1984, The effect of grain size on detrital modes: A test of the Gazzi-Dickinson point-counting method: Journal of Sedimentary Petrology, v. 54, p. 103–116.

Lai, S., and Zhang, G., 1996, Geochemical features of ophiolite in Mianxian-Lueyang suture zone, Qinling orogenic belt: China University of Geosciences Journal, v. 7, p. 165–172.

Lerch, M. F., Xue, F., Kroner, A., Zhang, G., and Todt, W., 1995, A middle Silurian–early Devonian magmatic arc in the Qinling Mountains of central China: Journal of Geology, v. 103, p. 437–449.

Li, C. Y., 1976, A preliminary analysis on the tectonic developments of some regions in China based on the plate tectonic theory: Acta Geophysical Sinica, v. 18, p. 52–76.

Li, C., Liu, Y., Zhu, B., Feng, Y., and Wu, H., 1978, Tectonic history of the Qinling and Qilian mountains, *in* Papers on geology for international exchange, Volume 1. Regional geology and geological mechanics: Beijing, China, Geological Publishing House, p. 174–187 (in Chinese).

Li, J., Cao, X., and Yang, J., 1994, Sedimentation and evolution of Phanerozoic oceanic basins in the Qinling orogenic belt: Beijing, China, Geological Publishing House, 206 p. (in Chinese).

Li, J., Niu, B., Liu, Z., Wang, Z., and Zhao, M., 1997, ^{40}Ar/^{39}Ar thermochronological evidence for the age of metamorphism and deformation of the Liziyuan Group on the northern side of the western section of the Qinling Mountains: Regional Geology of China, v. 16, p. 21–25 (in Chinese with English abstract).

Li, S., 1994, Implications of εNd-La/Nb, Ba/Nb, Nb/Th diagrams to mantle heterogeneity-classification of island arc basalts and decomposition of EMII composition: Geochimica, v. 23, p. 105–113.

Li, S., Hart, S. R., Zheng, S., Guo, A., Liu, D., and Zhang, G., 1989, Timing of collision between the North and South China blocks: Sm-Nd age evidence: Scientia Sinica, Series B., v. 32, p. 1393–1400.

Li, S., and Sun, W., 1995, A Middle Silurian–Early Devonian magmatic arc in the Qinling Mountains of central China: A discussion: Journal of Geology, v. 104, p. 501–503.

Li, S., Xiao, Y., Liou, D., Chen, Y., Ge, N., Zhang, S., Sun, S.-S., Cong, B., Zhang, R., Hart, S. R., and Wang, S., 1993, Collision of the North China and Yangtze blocks and formation of coesite-eclogites: Timing and processes: Chemical Geology, v. 108, p. 89–111.

Li, X., Yan, Z., and Lu, X., 1992, Granitoids of Qinling Dabie Mountains: Beijing, China, Geological Publishing House, 218 p. (in Chinese).

Li, Y., 1988, Primary exploration in the paleobiological division and palaeographic evolution during the Devonian period in the West Qinling: Journal of Xi'an Collage of Geology, v. 10, p. 14–18 (in Chinese with English abstract).

Li, Y., 1989, New advance on the Xihanshui Group: Northwest Geology, v. 3, p. 59–63 (in Chinese with English abstract).

Liang, Z., 1994, Geology, geochemistry, and tectonic setting of the Danfeng group metavolcanics in the Tianshui region, Gansu province: Acta Geologica Gansu, v. 3, p. 72–78 (in Chinese with English abstract).

Liu, B., Zhou, Z., Xiao, J., Chen, B., Zhao, X., Xin, J., Li, X., Du, Y., Xin, W., and Li, G., 1989, Characteristics of Devonian sedimentary facies in the Qinling Moutains and their tectono-paleogeographic significance: Journal of Southeast Asian Earth Science, v. 3, p. 211–217.

Marsaglia, K. M., 1991, Provenance of sands and sandstones from the Gulf of California, a rifted continental arc, *in* Fisher, R. V., and Smith, G. A., eds., Sedimentation in volcanic settings: Society of Economic Paleontologists and Mineralogists, Special Publication 45, p. 237–248.

Marsaglia, K. M., and Ingersoll, R. V., 1992, Compositional trends in arc-related, deep-marine sand and sandstone: A reassessment of magmatic-arc provenance: Geological Society of America Bulletin, v. 104, p. 1637–1649.

Matson, R. G., and Moore, G. F., 1992, Structural influences on Neogene subsidence in the central Sumatra forearc basin: American Association of Petroleum Geologists Memoir 53, p. 157–181.

Mattauer, M., Matte, P., Malavieille, J., Tapponnier, P., Maluski, H., Xu, Z., Lu, Y., and Tang, Y., 1985, Teconics of the Qinling belt: Build-up and evolution of eastern Asia: Nature, v. 317, p. 496–500.

Matte, Ph., Topponnier, P., Arnaud, N., Bourjot, L., Avouac, J. P., Vidal, Ph., Liu, Q., Pan, Y. S., and Wang, Y., 1996, Tectonics of western Tibet, between the Tarim and the Indus: Earth and Planetary Science Letters, v. 142, p. 311–330.

McLennan, S. M., Taylor, S. R., McCulloch, M. T., and Maynard, J. B., 1990, Geochemical and Nd-Sr isotopic composition of deep-sea turbidites: Crustal evolution and plate tectonic associations: Geochimica et Cosmochimica Acta, v. 54, p. 2015–2050.

Meng, Q., Men, Z., and Cui, Z., 1995, Reorganization of a missing Late Paleozoic old land in the northern margin of the South Qinling: Chinese Science Bulletin, v. 40, p. 254–256 (in Chinese).

Meng, Q., Xue, F., Zhang, G., 1994, Conglomerate sedimentation and its tectonic implication, Heihe area within the Shangdan zone of the Qinling: Acta Sedimentologica Sinica, v. 12, p. 37–45.

Meng, Q., Yu, Z., and Mei, Z., 1997, Sedimentation and development of the forearc basin at southern margin of the North Qinling: Scientia Geologica Sinica, v. 32, p. 136–145.

Meng, Q., and Zhang, G., 1999, Timing of collision of the North and South China blocks: Controversy and reconciliation: Geology, v. 27, p. 123–126.

Meng, Q., and Zhang, G., 2000, Geologic framework and tectonic evolution of the Qingling orogen, Central China: Tectonophysics, v. 323, p. 183–196.

Miall, A. D., 1996, The geology of fluvial deposits: New York, NY, Springer Verlag, 586 p.

Nemec, W., and Steel, R. J., 1984, Alluvial and coastal conglomerates: Their significant features and some comments on gravelly mass-flow deposits, *in* Koster, E. H., and Steel, R. J., eds., Sedimentology of gravel and conglomerates: Calgary, Alberta, Canada Society of Petroleum Geologists, Memoir 10, p. 1–31.

Niu, B., Fu, Y., Liu, Z., Ren, J., and Chen, W., 1994, Main tectonothermal events and $^{40}Ar/^{39}Ar$ dating of the Tongbai-Dabie Mts.: Acta Geoscience Sinica, v. 14, p. 20–34.

Okay, A. I., Sengör, A. M. C., and Stair, M., 1993, Tectonics of an ultra-high-pressure metamorphic terrane: The Dabie Shan/Tongbai Shan orogen, China: Tectonics, v. 12, p. 1320–1334.

Puchkov, V. N., 1997, Structure and geodynamics of the Uralian orogen, *in* Burg, J.-P., and Ford, M., eds., Orogeny through time: Geological Society of London, Special Publication 121, p. 201–236.

RGS Henan, 1989, Regional geology of Henan Province: Beijing, China, Geological Publishing House (in Chinese).

Ratschbacher, L., Hacker, B. R., Calvert, A., Webb, L. E., Grimmer, J. C., McWilliams, M. O., Ireland, T., Dong, S., and Hu, J., 2003, Tectonics of the Qinling (Central China): Tectonostratigraphy, geochronology, and deformation history: Tectonophysics, v. 366, p. 1–53.

Reischmann, T., Kröner, A., Sun, Y., Yu, Z., and Zhang, G., 1990, Opening and closure of an early Paleozoic ocean in the Qinling orogenic belt, China: Terra Abstracts, v. 2, p. 55–56.

Roger, F., Arnaud, N., Gilder, S., Tapponnier, P., Jolivet, M., Brunel, M., Malavieille, J., Xu, Z., and Yang, J., 2003, Geochronological and geological constraints on Mesozoic suturing in east-central Tibet: Tectonics, v. 22, p. 1037 [doi:10.1029/2002TC001466].

Schwab, M., Ratschbacher, L., Siebel, W., McWilliams, M., Minaev, V., Lutkov, V., Chen, F., Stanek, K., Nelson, B., Frisch, W., and Wooden, J. L., 2004, Assembly of the Pamirs: Age and origin of magmatic belts from the southern Tien Shan to the southern Pamirs and their relation to Tibet: Tectonics, v. 23, p. TC4002 [doi:10.1029/2003TC001583].

Song, H., Yu, Z., and Meng, Q., 1995, Sedimentary-tectonic setting of Heishan meta-sedimentary rocks series in the Shangzhou-Danfeng belt, East Qinling: Acta Petrologica Sinica, v. 11, p. 193–202.

Song, Z., Feng, Y., He, S., Li, Z., Zhao, L., and He, F., 1996, Isotopic chronology and geological significance of the Jiuciliang granite in the West Qinling mountains: Northwest Geoscience, v. 17, p. 6–10 (in Chinese with English abstract).

Song, Z., Jia, Q., Zhang, Z., and Zhang, M., 1991, The early Paleozoic volcanic rock series and its interconnection relationship between the North Qinling and the North Qilian orogens: Bulletin of Xi'an Institute of Geological Mineral Research, Chinese Academy of Geological Sciences, no. 34, p. 1–72 (in Chinese with English abstract).

Sun, W., Li, S., Sun, Y., Zhang, G., and Zhang, Z., 1996, Chronology and geochemistry of a lava pillow in the Erlangping Group at Xixia in the northern Qinling Mountains: Geology Reviews, v. 42, p. 144–153 (in Chinese with English abstract).

Wang, J. L., He, B. X., and Li, J. Z., eds., 1996, Zinling-type lead-zince deposits in China: Beijing, China, Metallurgical Publishing House, p. 79–153 (in Chinese with English abstract).

Wang, S., 1995, The geochemical features of the of the Yaolinghe Group and its significance: Geology of Hunan, v. 9, p. 72–83 (in Chinese with English abstract).

Wang, T., 2003, Characters of the accretionary wedge in the southwest margin of the West Qinling orogen: Unpublished M.Sc. thesis, Institute of Geology, Chinese Academy of Geological Sciences, 54 p.

Wang, Z. Q., Chen, H. H., and Hao, J., 1999, Preliminary determination of a Late Paleozoic and Triassic forearc accretionary wedge in the South Qinling, *in* Chen, H., Hou, Q., and Xiao, W., eds., Collision orogenic belts: Beijing, China, Marine Press, p. 100–113 (in Chinese with English abstract).

Wang, Z. Q., Wang, T., Yan, Z., and Yan, Q. R., 2002, Late Paleozoic fore-arc accretionary piggyback type basin system in the south Qinling, Central China: Geological Bulletin of China, v. 21, p. 456–464 (in Chinese with English abstract).

Xiao, P., Zhang, J., and Wang, H. 1999, The correlational study of various periods of volcanic rocks in the Tangzang-Huangbaiyuan tectonic belt in the Fengtai area, Shannxi province: Geology of Shannxi, v. 17, p. 33–41 (in Chinese with English abstract).

Xiao, W. J., Han, F. L., Windley, B. F., Yuan, C., Zhou, H., and Li, J. L., 2003, Multiple accretionary orogenesis and episodic growth of continents: Insights from the Western Kunlun Range, Central Asia: International Geology Review, v. 45, 303–328.

Xiao, W. J., Windley, B. F., Chen, H., Zhang, G. C., and Li, J. L., 2002a, Carboniferous–Triassic subduction and accretion in the western Kunlun, China: Implications for the collisional and accretionary tectonics of the northern Tibetan plateau: Geology, v. 30, p. 295–298.

Xiao, W. J., Windley, B. F., Hao, J., and Li, J. L., 2002b, Arc-ophiolite obduction in the Western Kunlun Range (China): Implications for the Palaeozoic evolution of central Asia: Journal of the Geological Society, London, v. 159, p. 517–528.

Xue, F., Kröner, A., Reischmann, T., and Lerch, F., 1996a, Paleozoic pre- and post-collision calc-alkaline magmatism in the Qinling orogenic belt, central China, as documented by zircon ages on granitiod rocks: Journal of the Geological Society, London, v. 153, p. 409–417.

Xue, F., Lerch, M. F., Kröner, A., and Reischmann, T., 1996b, Tectonic evolution of the east Qinling Mountains, China, in the Paleozoic: A review and new tectonic model: Tectonophysics, v. 253, p. 271–284.

Yan, Z., ed., 1985, Granitic rocks in Shaanxi Province, China: Xi'an, China, Xi'an Jiaotong University Press, 321 p. (in Chinese with English abstract).

Yan, Z., 2002, Sedimentation and metallization of the late Paleozoic fore-arc basin in the Western Qinling orogenic belt: Unpubl. Ph D. Thesis, Chinese Academy of Sciences, Beijing, 116 p.

Yang, Z., 1999, The accretional forearc structural zone and its evolutional analysis in late Paleozoic in the middle part of the Qinling area: Shaanxi Geology, v. 17, p. 1–6 (in Chinese with English Abstract).

Ye, K., Cong, B. L., and Ye, D. N., 2000, The possible subduction of continental material to depths greater than 200 km: Nature, v. 407, p. 734–736.

Ye, L., and Guan, S., 1944, Bulletin of geology, central southern part of Gansu Province: Special Papers on Geology, no. 19, 72 p. (in Chinese).

Yin, A., and Nie, S., 1993, An indentation model for the north and south China collision and the development of the Tanlu and Honam Fault systems, eastern Asia: Tectonics, v. 12, p. 801–813.

Yin, H., and Huang, D., 1995, The Early Paleozoic Zhen'an-Xichuan block and evolution of the small Qinling archipelagic ocean basin: Acta Geologica Sinica, v. 69, p. 193–204 (in Chinese with English abstract).

Yu, Z., and Meng, Q., 1997, Late Paleozoic sedimentary and tectonic evolution of the Shangdan suture zone, Eastern Qinling, China: Journal of Southeast Asian Earth Sciences, v. 11, p. 237–242.

Yu, Z., Sun, Y., Zhang, C., 1991, Geochemistry and tectonic setting of Shangdan graywacke in the Qinling orogenic belt, China: Geological Review, v. 37, p. 492–570 (in Chinese with English abstract).

Zhai, X., Day, H. W., Hacker, B. R., and You, Z. D., 1998, Paleozoic metamorphism in the Qinling orogen, Tongbai Mountains, central China: Geology, v. 26, p. 371–374.

Zhang, B., Luo, T., Gao, S., Quyang, J., Han, Y., and Gao, C., 1994, Geochemical constrains on the evolution of North China and Yangtze blocks: Journal of Southeast Asian Earth Science, v. 9, p. 405–416.

Zhang, C., Meng, Q., Yu, Z., and Zhang, G., 1997, Geochemical characteristics and tectonic implication of gravels in the Hubaohe conglomerates in the East Qinling: Acta Sedimentologica Sinica, v. 15, p. 115–119 (in Chinese with English abstract).

Zhang, E., Niu, D., Huo, Y., Zhang, L., and Li, Y., eds., 1993, Geologic-tectonic features of Qinling-Dabashan Mountains and adjacent regions: Beijing, China, Geological Publishing House, 291 p. (in Chinese with English abstract).

Zhang, G., Meng, Q., and Lai, S., 1995, Tectonics and structures of the Qinling orogenic belt: Science in China, v. B38, p. 1397–1386.

Zhang, G., Meng, Q., Yu, Z., Sun, Y., Zhou, D., and Guo, A., 1996, Orogenic processes and dynamics of the Qinling: Science in China, v. 39, p. 225–234 (in Chinese with English abstract).

Zhang, G., Su, Y., Yu, Z., and Xue, F., 1988, The ancient active continental margin of the northern Qinling orogenic belt, *in* Zhang G., ed., Formation and evolution of the Qinling orogen: Xi'an, China, Northwest University Press, p. 48–64 (in Chinese with English abstract).

Zhang, G., Yu, Z., Sun, Y., Cheng, S., Li, T., Xue, F., and Zhang, C., 1989, The major suture zone of the Qinling orogenic belt: Journal of Southeast Asian Earth Science, v. 3, p. 63–76.

Zhang, H., Gao, S., Zhang, B., Luo, T., and Lin, W., 1997, Pb isotopes of granitoids suggest Devonian accretion of Yangtze (South China craton to North China craton): Geology, v. 25, p. 1015–1018.

Zhang, W., and Meng, X., eds., 1994, Tectonic characteristics and orogenic process in the join of the Qilian–North Qinling orogenic belts: Xi'an, China, Northeast University Press, 283 p. (in Chinese with English abstract).

Zhang, Z., Liu, D., and Fu, G., 1991, Ages of the Qinling, Kuanping, and Taowan Groups in the North Qinling orogenic belt, middle China and their implications, *in* Ye, L., Qian, X., and Zhang, G., eds., A selection of papers presented at the Conference on the Qinling Orogenic Belt: Xi'an, China, Northwest University Press, p. 214–228 (in Chinese with English abstract).

Zhang, Z., Liu, D., and Fu, G., 1994, Isotopic geochronology of metamorphic rocks in the North Qinling orogenic belt: Beijing, China, Geological Publishing House, 231 p. (in Chinese with English abstract).

Zhang, Z., Zhang, G., Fu, G., Tang, S., and Song, B., 1996, Geochronology of metamorphic strata in the Qinling Mountains and its tectonic implications: Science in China, v. 39, p. 283–292.

Zhao, Z., Wan, Y., Zhang, S., and Wei, C., 1995, The geochemical features of the Douling metamorphic complex: Acta Petrologica Sinica, v. 11, p. 148–159 (in Chinese with English abstract).

Zhou, D., Zhang, C., Han, S., Zhang, Z., and Dong, Y., 1995, Tectonic setting of the two different tectonic-magmatic complexes of the East Qinling in the Early Paleozoic: Acta Petrologica Sinica, v. 11, p. 115–126 (in Chinese with English abstract).

Zhou, D., Zhang, C., Hua, H., and Hu, J., 1998, New knowledge about division and correlation of the Mid- and Neo-Proterozoic strata in the South Qinling: Geological Journal of China Universities, v. 4, p. 350–357.

Zhou, Z., Li, X., Wang, C., Li, X., and Liu, G., 1992, Clastic shelf sedimentary characters of the Devonian Liuling Group in the northern belt of Qinling, *in* Liu, B., Xiao, J., and Zhou, Z., eds., A selection of papers on the sedimentary geology of the Paleo-continental passive margin: Wuhan, China, China University of Geosciences Press, p. 11–24 (in Chinese with English abstract).

APPENDIX 1. Raw Point-Count Data

Location	Strata	Sample	N	Qm	Qp	P	K	Lvv	Lvf	Lvmi	Lvl	Lvp	Lmv	Lmm	Lmt	Lma	Lmp	Lsa	Lsc	Lsch	Lsi	M	D	Carb	Misc
Dacaotan Village	Dacaotan Group	B001	448	88	16	47	54	0	3	50	11	0	14	14	42	0	49	0	0	51	2	2	1	2	2
		B002	254	61	10	22	47	0	2	9	2	0	0	1	34	0	23	0	0	39	0	0	0	4	0
		B003	517	100	44	40	130	0	2	23	5	0	7	5	64	0	37	2	0	48	10	0	0	0	0
		B004	355	65	42	26	9	0	1	44	4	0	13	2	55	0	41	1	2	47	3	0	0	0	0
		B005	252	42	25	20	11	0	0	33	3	5	8	0	21	0	10	24	0	38	10	0	0	0	2
		B009	250	40	24	23	13	0	8	29	7	0	8	0	34	2	18	2	0	31	5	3	2	0	0
		B019	417	55	23	62	62	0	7	40	10	1	11	7	40	2	37	3	0	42	9	5	1	0	2
		B020	477	67	24	126	58	0	7	19	13	4	6	0	50	7	50	3	1	20	12	5	2	3	0
		B024	421	86	31	45	36	0	10	66	9	3	23	0	33	2	25	4	0	29	4	5	0	6	4
		B025	466	68	17	76	26	0	10	40	15	6	20	6	53	7	42	7	0	52	18	1	0	0	2
		B032	385	79	30	39	16	0	8	42	25	0	27	0	43	3	29	0	0	37	2	3	1	0	1
		B033	506	98	24	69	30	0	9	56	28	4	22	4	57	3	33	6	0	39	10	8	3	1	2
		B1094	289	55	15	81	28	0	5	25	2	0	8	0	7	1	31	1	0	19	1	10	0	0	0
Lixian	Shujiaba Group	B057	170	40	4	32	32	0	0	2	1	0	2	6	31	0	3	0	0	10	1	5	0	1	0
		B058	293	39	37	27	5	0	4	29	10	0	0	0	71	2	1	0	4	44	6	6	5	3	0
		B061	252	42	21	10	3	2	0	21	2	0	0	0	82	9	3	0	0	52	2	0	0	0	3
		B062	280	52	17	29	10	0	4	11	1	0	0	1	67	24	1	0	0	49	8	6	0	0	0
		B069	191	48	4	51	26	0	0	0	0	0	0	5	0	17	14	0	0	23	0	1	0	2	0
		B071	234	36	12	36	11	0	2	19	3	0	0	2	40	14	6	1	0	37	6	6	0	0	3
		B072	200	20	18	29	10	0	3	13	4	0	0	2	41	7	1	1	0	29	4	8	0	0	0
Xihe	Shujiaba Group	B084	87	15	2	20	16	0	0	0	0	0	0	0	12	0	0	0	0	13	0	0	0	9	0
		B092	117	18	3	33	28	0	0	0	0	0	0	0	4	0	17	0	0	8	0	6	0	0	0
		B093	132	17	5	14	36	0	2	8	4	0	2	0	14	0	9	0	0	17	0	2	0	0	2
		B094	55	10	3	8	4	0	0	0	0	0	0	0	0	0	8	0	0	15	0	0	0	7	0
		B095	71	13	5	16	19	0	1	5	2	0	0	1	0	7	1	0	0	0	0	1	0	0	0

Table continues

APPENDIX 1. *Continued*

Location	Strata	Sample	N	Qm	Qp	P	K	Lvv	Lvf	Lvmi	Lvl	Lvp	Lmv	Lmm	Lmt	Lma	Lmp	Lsa	Lsc	Lsch	Lsi	M	D	Carb	Misc
Xihe	Shujiaba Group	B096	69	17	2	13	10	0	0	0	0	0	0	1	10	0	4	0	0	12	0	0	0	0	0
		B098	250	48	4	61	56	0	0	0	0	0	5	5	32	0	19	0	0	15	2	3	0	0	0
Wushan	Dacaotan Group	B0121	408	92	20	12	2	1	6	71	10	2	24	3	43	4	39	3	0	64	4	5	1	0	2
		B0122	333	82	18	32	33	0	7	28	2	0	9	0	40	3	35	1	0	25	7	9	0	2	0
		B0123	325	63	19	72	34	0	3	9	2	1	10	1	35	8	33	1	0	8	14	6	1	0	5
Shixia	Xihanshui Group	B1020	151	32	4	24	19	0	0	4	0	0	4	0	26	0	21	1	0	12	0	0	0	4	0
Lixian	Dacaotan Group	B1043	282	42	21	56	38	0	2	6	4	0	4	6	60	0	0	0	0	32	0	4	0	3	0
		B1044	253	59	10	37	39	0	0	0	0	0	3	3	56	0	6	0	0	39	0	0	1	0	0
		B1057	252	38	39	7	2	0	6	48	10	0	0	5	46	3	3	1	0	40	3	1	0	0	0
		B1058	256	29	36	32	21	0	0	36	0	0	1	0	49	0	1	0	0	53	0	0	0	0	0
		B1059	402	50	22	33	31	0	4	47	15	2	10	5	42	2	49	2	0	27	7	2	0	3	0
Zhangxian	Dacaotan Group	B1062	423	64	16	87	80	0	2	32	9	3	3	1	35	0	28	2	0	48	8	3	2	0	0
		B1067	526	54	36	46	41	0	14	68	19	7	24	4	55	4	46	12	0	82	10	2	1	0	1
		B1074	435	92	33	38	15	1	10	64	5	11	16	2	52	7	25	2	0	47	8	4	0	1	2
		B1075	434	54	29	36	43	0	14	64	10	0	0	0	49	9	26	5	10	57	9	10	0	9	0
		B1076	515	58	27	84	97	0	3	43	11	1	8	8	44	5	54	3	0	55	7	6	1	0	0
		B1078	422	90	31	58	40	4	11	50	3	0	0	0	52	3	14	14	0	43	6	0	1	2	0
		B1080	281	42	19	39	51	0	3	27	6	0	6	0	31	2	12	4	0	35	4	0	0	0	0
Minxian Niuchang	Xihanshui Group	B1085	291	39	19	39	14	3	5	40	5	0	0	5	47	6	11	3	6	23	11	4	0	7	4
		B1087	282	59	14	34	12	0	7	31	3	0	2	0	50	9	8	3	5	29	11	5	0	0	0
		B1088	275	53	15	23	6	6	16	31	4	0	3	1	41	8	3	1	10	32	16	3	2	1	0
		B1089	285	34	17	58	22	14	20	14	13	3	2	6	8	16	0	4	0	26	10	7	3	5	3
		B1090	348	29	18	70	22	36	5	16	13	7	4	14	18	17	34	0	9	34	0	0	2	0	0

APPENDIX 2. Recalculated Parameters

Location	Strata	Sample	QFL%			QmFLt%			QmPK%			LmLvLs%			LvfLvmiLvl%		
			Q	F	L	Qm	F	Lt	Qm	P	K	Lm	Lv	Ls	Lvf	Lvmi	Lvl
Dacaotan Village	Dacaotan Group	B001	23.1	24.6	52.3	27.0	34.2	38.8	46.6	24.9	28.6	50.9	27.4	21.8	4.7	78.1	17.2
		B002	28.5	27.3	44.2	17.8	19.9	62.3	46.9	16.9	36.2	52.7	11.8	35.5	15.4	69.2	15.4
		B003	27.8	32.9	39.3	19.0	32.3	48.7	37.0	14.8	48.1	58.5	15.5	25.9	6.7	76.7	16.7
		B004	30.1	9.9	60.0	23.5	12.6	63.9	65.0	26.0	9.0	52.9	23.3	23.8	2.0	89.8	8.2
		B005	26.8	12.4	60.8	18.8	13.9	67.3	57.5	27.4	15.1	27.5	28.9	43.7	0.0	91.7	8.3
		B009	28.3	15.9	55.8	13.0	11.7	75.3	52.6	30.3	17.1	44.6	31.7	23.7	18.2	65.9	15.9
		B019	18.9	30.2	50.9	13.9	31.4	54.7	30.7	34.6	34.6	48.5	29.0	22.5	12.3	70.2	17.5
		B020	19.5	39.4	41.1	13.7	37.6	48.7	26.7	50.2	23.1	62.8	23. 9	13.3	17.9	48.8	33.3
		B024	28.8	20.0	51.2	18.7	17.6	63.7	5.1	26.9	21.6	40.7	43.1	16.2	11.8	77.6	10.6
		B025	18.4	22.0	59.6	16.3	24.5	59.2	40.0	44.7	15.3	49.6	27.5	22.9	15.4	61.5	23.1
		B032	28.7	14.5	56.8	18.4	12.8	68.8	58.9	29.1	11.9	47.7	35.0	17.3	10.7	56.0	33.3
		B033	24.8	20.1	55.1	31.4	31.7	36.9	49.7	35.0	15.2	45.6	37.2	17.2	9.7	60.2	30.1
		B1094	25.1	39.1	35.8	24.5	48.7	26.8	33.5	49. 4	17.1	47.5	32.3	20.2	15.6	78.1	6.3
Lixian	Shujiaba Group	B057	26.8	39.0	34.2	12.8	20.5	66.7	38. 5	30.8	30.8	76.4	5.45	18.2	0.0	66.7	33.3
		B058	27.2	11.5	61.3	14.7	12.1	73.2	54.9	38.0	7.08	44.8	26.1	29.1	9.3	67.4	23.3
		B061	25.3	5.2	69.5	17.6	5.5	76.9	76.4	18. 2	5.5	55.0	14.6	30.4	0.0	91.3	8.7
		B062	25.2	14.2	60.6	33.8	25.3	40.9	57.1	31.9	11.0	58.9	10.1	31.0	25.0	68.8	6.3
		B069	27.7	41.0	31.3	17.9	28.8	53.3	38.4	40.8	20.8	61.0	0.0	39.0	0.0	0.0	0.0
		B071	21.3	20.9	57.8	16.8	21.9	61.3	43.3	43.4	13.3	50.0	19.4	30.6	8.3	79.2	12.5
		B072	20.0	20.5	59.5	23.2	45.3	31.5	33.9	49.2	16.9	50.5	19.8	29.7	15	65.0	20.0
Xihe	Shujiaba Group	B084	21.7	46.2	32.1	16.9	40.4	42.7	29.4	39.2	31.4	48.0	0.0	52.0	0.0	0.0	0.0
		B092	17.9	52.1	30.0	8.8	29.8	61.5	22.8	41.8	35.4	72.4	0.0	27.6	0.0	0.0	0.0
		B093	17.3	39.4	43.3	6.1	17.8	76.1	25.4	20.9	53.7	44.6	25.0	30.4	14.3	57.1	28.6
		B094	27.1	25.0	47.9	20.8	25.0	54.2	45. 5	36.4	18.2	0.0	34.8	65.2	0.0	0.0	0.0
		B095	25.7	50.0	24.3	18.6	50.0	31.4	27.1	33.3	39.6	47.1	52.9	0.0	12.5	62.5	25.0

Appendix continues

APPENDIX 2. *Continued*

Location	Strata	Sample	QFL% Q	QFL% F	QFL% L	QmFLt% Qm	QmFLt% F	QmFLt% Lt	QmPK% Qm	QmPK% P	QmPK% K	LmLvLs% Lm	LmLvLs% Lv	LmLvLs% Ls	LvfLvmiLvl% Lvf	LvfLvmiLvl% Lvmi	LvfLvmiLvl% Lvl
Xihe	Shujiaba Group	B096	27.5	33.3	39.1	24.6	33.3	42.0	42.5	32.5	25.0	55.6	0	44.4	0.0	0.0	0.0
		B098	21.1	47.3	31.6	19.4	47.4	33.2	29.2	36.9	33.9	78.2	0	21.8	0.0	0.0	0.0
Wushan	Dacaotan Group	B0121	28.0	3.5	68.5	23.0	3.5	73.5	86.8	11.3	1.9	41.3	32.8	25.9	6.9	81.6	11.5
		B0122	31.1	20.2	48.7	25.5	20.2	54.3	55.8	21.8	22.4	55.4	23.6	21.0	18.9	75.7	5.4
		B0123	26.2	33.9	39.9	20.1	33.9	46.0	37.3	42.6	20.1	69.6	12.0	18.4	21.4	64.3	14.3
Shixia	Xihanshui Group	B1020	24.5	29.3	46.2	21.8	29.3	48.9	42.7	32	25.3	75.0	5.9	19.1	0.0	100.0	0.0
Lixian	Dacaotan Group	B1043	23.2	34.7	42.1	15.5	34.7	49.8	30.9	41.2	27.9	61.4	10.5	28.1	16.7	50.0	33.3
		B1044	27.4	30.2	42.4	23.4	30.2	46.4	43.7	27.4	28.9	63.6	0.0	36.4	0.0	0.0	0.0
		B1057	30.7	3.6	65.7	15.1	3.6	81.3	80.9	14.9	4.3	34.5	38.8	26.7	9.4	75.0	15.6
		B1058	25.2	20.5	54.3	11.2	20.5	68.2	35.4	39.0	25.6	36.4	25.7	37.9	0.0	100.0	0.0
		B1059	20.7	18.4	60.9	14.4	18.4	67.2	43.9	28.9	27.2	50.9	32.1	17.0	6.1	71.2	22.7
Zhangxian	Dacaotan Group	B1062	19.1	40.0	40.9	15.3	39.9	44.8	27.7	37.7	34.6	39.2	26.9	33.9	4.7	74.4	20.9
		B1067	17.2	16.7	66.1	10.3	16.7	73.0	38.3	32.6	29.1	38.6	31.3	30.1	13.9	67.3	18.8
		B1074	29.2	12.4	58.4	21.5	12.4	66.1	63.4	26.2	10.3	40.8	36.4	22.8	12.7	81.0	6.33
		B1075	20.0	19.1	60.9	13.0	19.0	70.0	40.6	27.1	32.3	33.2	34.8	32.0	15.9	72.7	11.4
		B1076	16.7	35.6	47.6	11.4	35.6	53.0	24.3	35.1	40.6	49.2	23.9	26.9	5.3	75.4	19.3
		B1078	28.9	23.4	47.7	21.5	23.4	55.1	47.9	30.9	21.3	34.5	34.0	31.5	17.2	78.1	4.7
		B1080	21.7	32.0	46.3	14.9	32.0	53.0	31.8	29.5	38.6	39.2	27.7	33.1	8.3	75.0	16.7
Minxian Niuchang	Xihanshui Group	B1085	21.0	19.2	59.8	14.1	19.2	66.7	42.4	42.4	15.2	41.8	32.1	26.1	10.0	80.0	10
		B1087	26.4	16.6	57.0	21.3	16.6	62.1	56.2	32.4	11.4	43.7	25.9	30.4	17.1	75.6	7.3
		B1088	25.3	10.8	63.9	19.7	10.8	69.5	64.6	28.1	7.3	32.6	33.1	34.3	31.4	60.8	7.8
		B1089	19.1	30.0	50.9	12.7	30.0	57.3	29.8	50.9	19.3	23.5	47.1	29.4	42.6	29.8	27.7
		B1090	13.6	26.6	59.8	8.4	26.6	65.0	23.9	57.9	18.2	42.0	37.2	20.8	14.7	47.1	38.2

APPENDIX 3. Mean Recalculated Parameters

Location	Strata	Number of samples	QFL%			QmFLt%			QmPK%			LmLvLs%			LvfLvmiLvl%		
			Q	F	L	Qm	F	Lt	Qm	P	K	Lm	Lv	Ls	Lvf	Lvmi	Lvl
Dacaotan Village	Dacaotan Group	13	25.3	23.7	51	19.7	25.3	55.0	45.7	29.9	24.4	49.3	26.9	23.8	10.8	71.1	18.1
Lixian	Shujiaba Group	7	24.8	21.8	53.4	19.5	22.8	57.7	47.2	36.4	16.4	56.7	13.6	29.7	9.6	73.1	17.3
Xihe	Shujiaba Group	7	22.6	41.9	35.5	16.5	34.8	48.7	27.0	36.8	36.3	49.4	16.1	34.5	13.3	59.8	26.9
Wushan	Dacaotan Group	3	28.4	19.2	52.4	22.9	19.2	57.9	59.9	25.3	14.8	55.4	22.8	21.8	16.3	76.8	6.9
Shixia	Xihanshui Group	1	24.5	29.3	46.2	21.8	29.3	48.9	42.7	32	25.3	75.0	5.9	19.1	0.0	100.0	0.0
Lixian	Dacaotan Group	5	25.4	21.5	53.1	15.9	21.5	62.6	46.9	30.3	22.9	49.4	21.4	29.2	8.0	74.1	17.9
Zhangxian	Dacaotan Group	7	21.8	25.6	52.6	15.4	25.3	59.3	39.2	31.3	29.5	39.2	30.7	30.1	11.1	74.8	14.1
Minxian Niuchang	Xihanshui Group	5	21.1	20.6	58.3	15.2	20.6	64.2	43.4	42.3	14.3	36.7	35.1	28.2	23.2	58.6	18.2

APPENDIX 4. Geochemical Analysis Data for the Devonian Siltstones and Mudstone[1]

Sample	B26*	B32	B33	B34	B36	B1022	B1023	B085	B088	B1048	B1049	B1050	B1051	B1053	B1054	Hl1	HL2	HL3	HL4*	HL5*	WJ1#	WJ2#	WJ3#	WJ4#	WJ5#	WJ6#
Na_2O	0.12	0.32	0.25	1.27	1.38	1.3	0.7	0.8	0.82	2.72	0.85	1.23	1.44	2	0.82	1.34	0.95	1.5	0.52	0.52	0.27	0.62	0.79	0.91	0.66	2.18
MgO	2.8	1.5	1.68	3.5	3.64	2.65	2.47	2.53	2.4	3.51	3.56	3.62	3.37	3.62	2.99	3.49	5.52	2.6	1.14	2.93	3.95	1.39	3.57	2.71	2.23	3.26
Al_2O_3	17.62	20.73	20.08	18.77	19.12	17.73	20.04	20.34	16.88	12.15	12	17.71	18.1	19.12	11.89	22.49	18.31	17.32	20.78	18.51	14.86	6.58	15.26	11.3	13.24	10.39
SiO_2	59.4	61.21	61.7	59.75	59.41	59.01	59.62	58.92	60.06	59.7	47.44	56.58	60.59	59.16	53.02	60.63	58.14	59.76	66.11	63.24	54.39	74.44	54.29	61.71	54.49	58.75
P_2O_5	0.16	0.12	0.14	0.14	0.14	0.11	0.1	0.11	0.18	0.14	0.12	0.14	0.14	0.14	0.12	0.11	0.09	0.09	0.1	0.12						
K2O	5.02	5.23	5.49	4.09	4.03	3.91	4.72	4.43	6.7	3.24	2.47	4.16	3.53	3.85	2.54	4.16	5.49	3.78	6.31	5.24	4.00	1.87	3.82	2.67	2.89	1.169
CaO	0.96	<0.01	<0.01	<0.01	<0.01	2.3	0.44	0.58	2.46	6.18	13.68	0.28	0.27	0.44	11.11	0.2	3.51	3.45	0.44	0.73	4.39	4.86	7.44	7.14	10	11.32
TiO_2	0.84	0.82	0.85	0.82	0.82	0.77	0.84	0.81	0.84	0.64	0.54	0.73	0.78	0.78	0.56	0.61	1.42	0.47	0.88	0.74	0.46	0.85	0.71	0.56	0.57	0.58
MnO	0.12	0.02	0.02	0.05	0.05	0.04	0.04	0.04	0.05	0.09	0.07	0.04	0.06	0.04	0.09	0.08	0.05	0.02	0.02	0.03	0.04	0.03	0.07	0.06	0.06	0.08
Fe_2O_3	5.95	2.98	3.33	1.89	1.98	2.54	2.83	2.31	1.2	1.37	1.01	1.52	1.71	2.03	0.96	0.82	1.62	0.52	2.77	5.7	1.99	0.7	1.69	1.05	2.2	1.51
FeO	1.26	2.17	1.63	4.53	4.68	4.4	4.22	4.67	4.42	3.3	3.38	4.42	5.07	4.51	3.24	5.76	4.48	4.63	0.23	1.97	2.97	1.66	3.99	3.86	2.85	3.60
CO2	1.48	0.12	0.2	0.54	0.29	1.38	0.22	0.3	1.2	3.98	11.42	1.47	0.13	0.13	8.64											
H_2O^+	4.02	4.34	4.08	4.16	4.29	3.94	4.24	4.54	2.34	2.47	3.26	3.4	4.28	4.18	3.67											
Sums	99.75	99.56	99.45	99.51	99.83	100.08	100.48	100.38	99.55	99.49	99.8	95.3	99.47	100	99.65	99.69	99.58	94.14	99.3	99.73	87.32	93	91.63	91.97	81.19	92.84
Sc	17.4	19.5	21.4	18.2	19.4	15	17	13	19	14	13	17	19	16	14											
V	115	132	141	118	124	143	156	167	139	103	96	156	163	164	99											
Cr	118	127	144	129	120	106	98	85	82	66	64	102	114	108	68											
Co	19.9	13	12.5	14.8	14.6	23	12	17	28	16	19	13	16	9.8	16											
Ni	63.9	45.3	56.5	61.3	57.8	44	49	49	46	36	36	53	53	48	39											
Cu	6.89	17.5	16.1	12.1	13.8	16	6.7	29	50	10	29	0.3	0.5	0.8	5.7											
Zn	86.3	33.6	32	55.4	52.8	18	52	90	88	83	79	39	80	50	46											
Rb	215	255	283	174	179	132	158	107	230	124	121	97	105	76	128											
Sr	42.2	32.9	34.8	47.5	50.2	44	45	49	64	822	260	59	81	60	143											
Nb	18.6	16.8	19	17.1	17.7	12	14	16	14	11	9	11	14	12	9.7											
Cs	12.7	12.5	14.4	8.62	8.46	4.9	7.7	8.9	16	5.2	6	8.7	6.8	4.1	4.9											
Ba	708	598	1.19	567	568	556	411	339	1011	1928	404	407	322	453	418											
Ta	1.13	1.01	1.2	1.06	1.11	1.8	2.4	2.6	2.6	1.2	0.9	1.9	2.2	1.7	1											
Pb	16.9	7.13	5.61	3.51	4.33	4	4	6.8	17	60	13	3.9	5.2	4.8	5.8											
Th	14.7	15.3	17.7	15.2	16.2	16	14	11	19	15	13	12	13	11	13											
U	1.75	2.76	2.56	2.59	2.72	1.9	2	1.8	2.5	2.4	1.8	1.6	4	2.8	1.8											
Zr	171	134	148	154	139	148	149	145	190	168	94	139	154	154	108											
Hf	4.94	3.9	4.22	4.38	4.04	4.8	4.6	4	6.2	5.2	2.9	4.2	4.9	4.7	3.4											
La	45.4	46.7	52.4	48.7	44.9	42.23	40.27	42.53	42.97	32.65	29.1	41.04	43.04	41.48	27.3											
Ce	88.4	83.9	96.4	92.1	84.4	82.15	77.75	83.4	85.33	63.3	55.95	78.37	81.79	77.49	50.88											
Pr	10.3	10.5	12	11.2	10.1	8.258	7.882	8.412	8.367	6.253	5.644	8.018	8.652	80159	5.3											
Nd	37.8	37.9	41.7	40.1	36.3	32.58	30.79	33.65	32.18	25.97	22.1	32.15	33.45	32.27	20.4											
Sm	6.94	6.53	7.58	7.43	6.7	6.113	5.497	6.03	5.762	4.944	4.098	5.811	5.995	5.981	3.489											
Eu	1.3	1.16	1.18	1.34	1.21	1.42	1.245	1.39	1.23	1.032	0.881	1.29	1.382	1.412	0.799											
Gd	6.24	5.56	6.56	6.37	5.81	5.319	4.614	5.227	5.141	4.47	3.526	4.855	5.182	4.863	2.906											
Tb	0.92	0.78	0.92	0.92	0.87	1.039	0.86	0.951	1.028	0.83	0.388	0.898	0.605	0.78	0.198											
Dy	4.7	3.98	4.85	4.73	4.41	4.752	3.998	4.856	4.789	4.222	2.89	4.058	4.192	3.533	2.37											
Ho	0.99	0.83	1.01	0.98	0.93	0.866	0.688	0.883	0.89	0.785	0.476	0.715	0.661	0.596	0.408											
Er	2.91	2.44	2.98	2.91	2.72	2.61	1.945	2.67	2.827	2.307	1.511	2.188	2.097	1.601	1.179											
Tm	0.43	0.37	0.44	0.42	0.41	0.335	0.26	0.431	0.392	0.301	0.145	0.28	0.218	0.214	0.073											
Yb	2.85	2.46	2.93	2.88	2.7	2.6	1.793	2.753	2.894	2.272	1.421	1.939	2.018	1.705	1.067											
Lu	0.44	0.38	0.46	0.43	0.42	0.375	0.251	0.394	0.425	0.318	0.204	0.266	0.285	0.25	0.153											
Y	27.9	22.9	28.1	26.5	25.2	24.27	18.24	25.13	25.38	21.58	13.98	19.24	19.82	15.39	11.17											

[1]Major elements in wt %, trace elements in ppm; * = samples of the Dacaotan Group; # = samples of the Xihanshui Group; other samples represent the Xihanshui Group. HL1-5 data from Huo and Li, 1995; WJ1-6 data from Wang et al., 1996.